PHOTOCATALYTIC DEGRADATION OF CASSAVA WASTEWATER USING ACID-ACTIVATED CLAY-TiO_2 COMPOSITES UNDER UV-IRRADIATION

BY

OMOROTIONMWAN PRECIOUS DESTINY

ENG2003783

DEPARTMENT OF CHEMICAL ENGINERING

FACULTY OF ENGINEERING

UNIVERSITY OF BENIN

EDO STATE, NIGERIA

OCTOBER, 2025

PHOTOCATALYTIC DEGRADATION OF CASSAVA WASTEWATER USING ACID-ACTIVATED CLAY-TiO_2 COMPOSITES UNDER UV-IRRADIATION

BY

OMOROTIONMWAN PRECIOUS DESTINY

ENG2003783

A PROJECT SUBMITTED TO THE DEPARTMENT OF CHEMICAL ENGINEERING, UNIVERSITY OF BENIN, BENIN CITY, NIGERIA IN PARTIAL FULFILMENT OF THE REQUIREMENTS FOR THE AWARD OF BACHELOR OF ENGINEERING IN CHEMICAL

OCTOBER, 2025

CERTIFICATION

This is to certify that this research project was carried out by **OMOROTIONMWAN PRECIOUS DESTINY** with matriculation number **ENG2003783** in the Department of Chemical Engineering at the University of Benin, Benin city, Edo state Nigeria.

---------- ----------

Engr. Prof. F.E. AISIEN Date

Project Supervisor

---------- ----------

Engr. Prof. S.E. Uwadiae Date

Project Coordinator

---------- ----------

Engr. Prof. E. A. Oyedoh Date

Ag. Head of Department

---------- ----------

External Examiner Date

DEDICATION

This project work is dedicated to ALMIGHTY GOD, who has brought me thus far in this my academic journey, the source of my life and my everything. Special appreciation and dedication also to my parents**, Mr and Mrs OMOROTIONMWAN**, my uncle **Pharm.D NELSON UGOBOR** and my best friend **IRABOR AILUORIO JONATHAN** for their contribution and support financially, spiritually, morally in this journey, I wouldn't achieve this academic feat without them.

ACKNOWLEDGEMENT

I wish to express my profound gratitude to my project supervisor **Engr. Prof. F.E. AISIEN** for his help, support, timely correction and the bank of knowledge which he was willing to instill during the course of the project.

Also, as the HOD, Department of Chemical Engineering **Engr. Prof. E. A. Oyedoh** has shown awesome, great and tenacious leadership and guidance throughout the course of this project.

I'm also grateful to the lecturers for their tutoring which made my stay here a great one. A special appreciation to **Engr. Prof Ralph Edopkia** for being a great lecturer and friend to me. I will also want to appreciate the lab assistant in the department laboratory, in person of Mr. Collins and Engr. Moses whose support was also helpful.

I would like to express my profound gratitude to my Family; to my parents, **Mr & Mrs OMOROTIONMWAN** for their financial, moral, spiritual, and constant support all through my stay in school and my siblings (Gertrude, Blessing, Unity, Freedom and Godswill) whose love and prayer kept me going.

Special thanks to my friend **Chimuanya Anthony Egbeyi**, for his unwavering love and support financially and morally throughout my academic journey which I am very grateful for.

I also would also extend this hand of appreciation to my friends and colleagues, **Faith Benedict, Joseph Kennedy, Chidinma Abazie, Idah Paul** for being very supportive and making my academic years bearable.

ABSTRACT

The cassava processing industry produces large quantities of wastewater that is highly contaminating, marked by a severe organic load and the presence of toxic cyanide. This wastewater represents considerable threats to public health and the environment. Conventional treatment methods often lack efficiency or are too costly, particularly for small-scale processors. This study explored the creation and effectiveness of an economical, sustainable photocatalytic system based on acid-activated clay-TiO_2 composites for breaking down cassava wastewater when exposed to UV light.

Kaolin and bentonite clays from Auchi, Nigeria were sourced locally and their surface properties were enhanced through acid activation using 2M H_2SO_4. Using a direct impregnation method, composites were synthesized with TiO_2 (Degussa P25). Characterization of the materials with SEM, XRD, FTIR, and XRF confirmed successful acid activation, as demonstrated by increased porosity and surface area, along with the effective formation of the clay-TiO_2 composite. With a pH of 4.1, a COD of 32,000 mg/L, a BOD_5 of 18,500 mg/L, and a cyanide concentration of 50 mg/L, the raw cassava wastewater demonstrated significant pollution strength.

The photocatalytic degradation experiments assessed the influence of catalyst dosage, irradiation time, pH, and initial cyanide concentration. Under optimal conditions (catalyst dosage: 1.5 g/L, pH: 3.0, irradiation time: 180 min), the acid-activated Bentonite-TiO_2 composite achieved a maximum cyanide removal efficiency of 94.7%, surpassing that of the Kaolin-TiO_2 composite (88.9%). The kinetic analysis indicated that the degradation process adhered to a pseudo-first-order model, with the Bentonite-TiO_2 composite showing a higher apparent rate constant (0.0154 min^{-1}) than that of Kaolin-TiO_2 (0.0116 min^{-1}). The bentonite-based composite performs better due to its enhanced porosity, increased surface area, and improved TiO_2 dispersion, which together improve adsorption and photocatalytic degradation.

This research effectively shows that acid-activated clay-TiO_2 composites, especially those made with bentonite, serve as highly effective, economical, and environmentally friendly catalysts for cassava wastewater treatment, presenting a promising sustainable approach to pollution reduction in the agro-processing sector.

TABLE OF CONTENTS

LIST OF FIGURES

LIST OF TABLES

NOMENCLATURE

220AOP – Advanced Oxidation Process

BOD – Biochemical Oxygen DemandCCS – Carbon Capture and Storage

127COD – Chemical Oxygen Demand

DO – Dissolved Oxygen

EDX – Energy Dispersive X-ray Spectroscopy

145FTIR – Fourier Transform Infrared Spectroscopy

IGCC – Integrated Gasification Combined Cycle

NSDWQ – Nigerian Standard for Drinking Water Quality

193OECD – Organization for Economic Co-operation and Development

119pH – Measure of acidity or alkalinity of a solutionPPM – Parts Per Million (concentration unit)

99SEM – Scanning Electron MicroscopyTDS – Total Dissolved Solids

TSS – Total Suspended Solids

XRD – X-ray Diffraction

CHAPTER 1

INTRODUCTION

BACKGROUND OF THE STUDY

Cassava (Manihot esculenta Crantz) is a major food security crop in Sub-Saharan Africa, supporting nearly 200 million people as their principal carbohydrate supply (FAO, 2013). Cassava roots must be processed into shelf-stable products because the crop deteriorates quickly after harvest, with roots becoming unmarketable within 48-72 hours (Westby, 2002). Traditional processing methods have evolved throughout regions to meet both preservation needs and cyanogenic glycoside reduction, which, if not correctly treated, can result in konzo (Bokanga, 1994). Peeling begins the processing chain and is normally done manually with knives, while automated peelers have been used in some commercial operations (Adekanye et al., 2013). The following fermentation stage varies greatly across regions: in West Africa, submerged fermentation for 3-5 days generates distinctive products such as garri (Oyewole, 2001), whereas heap fermentation for 2-3 days is predominant in East Africa (Nambisan, 2011). Fermentation techniques reduce cyanide content to safe levels (<10 ppm) while also improving functional characteristics and micronutrient absorption (Montagnac et al., 2009). Sun-drying is the most common preservation method, although studies show it can result in 15-30% nutritional loss, especially vitamin C and β-carotene (Bradbury & Holloway, 1988). The dry chips are frequently processed into flour using hammer mills or disc attrition mills, with particle size distribution influencing product quality (Sanni et al., 2009). Recent innovations in flash drying technology have enabled production of high-quality cassava flour (HQCF) with less than 10% moisture content, meeting international standards for industrial applications (Aryee et al., 2006).

Value addition through starch extraction has become commercially important, with Nigeria producing roughly 300,000 metric tons per year for diverse industrial uses (Oguntunde 2005). Ethanol production from cassava has increased dramatically, particularly in Ghana and Nigeria, where government policies encourage biofuel ventures. Other novel products include fortified cassava flour with increased protein content from soybean or groundnut addition (Eggleston et al., 1992) and precooked composite flours for supplemental foods (Temple & Badamosi, 2016).

Despite technical advances, substantial difficulties remain. Due to poor processing facilities, postharvest losses continue to be substantial at 25-40% (Adeniji et al., 2011). Energy needs for automated processing provide economic hurdles, with small-scale processors spending up to 40% of their production costs on fuel (Igbeka et al., 2009). Furthermore, fluctuating product quality and food safety concerns continue to hinder export opportunities (Tomlins et al., 2007). Recent biotechnology advancements offer intriguing options, such as low-cyanide cassava varieties that require less processing (Sayre et al., 2011). Mobile processing units have improved rural technology access (Adekanye et al., 2015), whereas cooperative models have increased smallholder market access (Abass et al., 2014). Policy interventions like Nigeria's Cassava Transformation Agenda show how focused support can lead to sector-wide growth (Phillips et al., 2004).

Cassava processing generates large amounts of wastewater, which poses both environmental issues and significant opportunities for resource recovery. This liquid effluent, also known as cassava mill effluent (CME), is produced during the production of garri, fufu, starch, and other cassava derivatives through a variety of processing phases such as washing, soaking, fermentation, and pressing. The content of this wastewater varies greatly depending on the processing method, but

inappropriate disposal has been related to substantial environmental degradation and public health concerns in several African cassava-producing countries (Ubalua and Ezeronye, 2007).

Cassava wastewater's physicochemical parameters highlight its complexity and potential environmental impact. The effluent contains substantial organic content, with COD values ranging from 15,000 to 50,000 mg/L and BOD_5 values ranging from 8,000 to 25,000 mg/L (Adelekan & Bamgboye, 2009; Nwabueze & Otunwa, 2016). These data show an organic pollution load that is 200-300 times higher than ordinary home sewage, which explains the significant impact on receiving aquatic bodies. The wastewater also contains significant suspended particles (1,500–5,000 mg/L), which contribute to turbidity and sedimentation in aquatic habitats (Oti et al., 2020). Another important property is acidity, which normally ranges between 3.5 and 5.0 due to the presence of organic acids produced during fermentation such as lactic, acetic, and formic acids (Oboh & Akindahunsi, 2003). This low pH not only causes corrosion in infrastructure, but it also generates unfavorable environmental conditions for aquatic life. The wastewater's abnormally high organic load produces severe oxygen deprivation, which disproportionately affects aquatic habitats. According to research, the biological oxygen demand (BOD) from a single medium-sized processing unit can entirely deplete dissolved oxygen in large water volumes, resulting in mass fish mortality and ecosystem collapse (Adelekan and Bamgboye, 2009). Rural communities who rely on these bodies of water for fishing are seeing a decline in catches, while eutrophication induced by nutrient-rich effluent causes algal blooms that disrupt entire aquatic food systems (Nwoko & Ogunyemi, 2010; Ogunniyi et al., 2019). When wastewater is released onto land, the repercussions for terrestrial environments are equally severe. The effluent's acidic pH changes soil chemistry, affecting fertility and crop yields by 30-40% in impacted areas (Eze et al., 2015; Oshoma et al., 2017). Cyanide chemicals remain in these soils, causing long-term pollution that

affects microbial populations and nutrient cycling (Ahaotu et al., 2013). These consequences exacerbate current agricultural issues in areas where cassava is a staple crop and an economic mainstay.

Human health consequences emerge from a variety of exposure mechanisms. Direct contact with cyanide-laden wastewater produces acute poisoning in processors, whereas prolonged exposure via polluted water sources causes neurological illnesses such as konzo (Cliff et al., 2011; Nhassico et al., 2008). Stagnant wastewater pools serve as breeding grounds for disease vectors, raising malaria and waterborne illness rates in local communities (Okafor et al., 2018). The economic implications are felt throughout affected regions, with losses in fisheries, agriculture, and increased healthcare costs perpetuating cycles of poverty and food insecurity (Nwoko & Ogunyemi, 2010; Eze et al., 2015).

The environmental impact of untreated cassava wastewater discharge is significant and well-documented.

Innovative techniques to wastewater treatment are emerging in Africa's cassava processing industries. Biogas technology adoption has yielded excellent results, with methane concentration reaching 60-70% in optimised systems (Ofoefule et al. 2010). Agricultural uses show promise after cyanide removal, with research demonstrating higher crop yields when adequately treated wastewater is utilized for irrigation (Eze et al., 2015). Industrial applications include starch recovery for glue manufacture and ethanol synthesis via microbial fermentation (Nwabueze & Otunwa, 2016; Ahaotu et al., 2013).

The conversion of cassava wastewater from an environmental problem to a lucrative resource necessitates collaborative efforts from many sectors. Policy interventions should prioritize the development of cost-effective treatment technologies for small-scale processors, who account for

the vast majority of cassava operations in Africa. Research institutions must continue to develop effective cyanide detoxification strategies while also investigating novel valorization pathways. Extension programs play an important role in promoting best wastewater management techniques among rural processors. Cassava wastewater, with proper treatment and utilization, has the potential to greatly contribute to circular economy models in Africa's agricultural sector while decreasing its existing environmental impact.

The disposal of untreated cassava wastewater is a complicated dilemma in Africa's cassava-producing regions, with implications ranging from environmental degradation to public health concerns and economic losses. Small-scale processing enterprises, which dominate the industry, frequently release this effluent directly into nearby ecosystems, resulting in cumulative effects that endanger both natural systems and human communities (Ubalua and Ezeronye, 2007).

These issues remain due to various hurdles such as technical limitations, economic constraints, and policy deficiencies. Small-scale processors, who form the industry's backbone, frequently lack access to cost-effective treatment methods capable of handling the wastewater's specific properties (Nwabueze & Otunwa, 2016). The seasonal pattern of processing hinders investment in treatment infrastructure, while lax enforcement of environmental legislation allows for continued unsustainable practices (Ofoefule et al., 2010; Ogunniyi et al., 2019). Emerging solutions focus on circular economy concepts that convert wastewater from a burden to a resource.

Photocatalysis has evolved as a strong technique that uses light energy to power chemical reactions, providing long-term solutions for environmental remediation and renewable energy production. This method uses semiconductor materials that, when lighted, produce electron-hole pairs capable of decomposing contaminants, producing clean hydrogen fuel, and purifying air and

water. Growing global concerns about water pollution, air quality, and energy sustainability have positioned photocatalysis as an environmentally friendly alternative to traditional treatment methods, particularly for persistent organic pollutants and industrial effluents that resist biological degradation (Chong et al., 2010). Photocatalysis occurs when photons with enough energy excite electrons in semiconductor materials, causing charge carriers to migrate to the surface and engage in redox reactions (Linsebigler et al., 1995). These photogenerated electrons and holes interact with surrounding molecules to form highly reactive species like hydroxyl radicals, which can convert complex organic pollutants into innocuous compounds like carbon dioxide and water (Hoffmann et al., 1995). Titanium dioxide remains the most extensively investigated photocatalyst because to its stability, non-toxicity, and good electrical characteristics, but its reliance on UV light activation has prompted research into modified and alternative materials (Hashimoto et al., 2005).

In environmental applications, photocatalysis is extremely effective for wastewater treatment, particularly for difficult pollutants such cyanide compounds found in cassava processing effluent (Adewuyi, 2020). Researchers in Africa have made significant contributions to this field by developing solar-driven systems that use modified titanium dioxide and locally available materials to achieve complete cyanide removal and organic load reduction under natural sunlight conditions (Boakye et al., 2019; Oluwafemi et al., 2019). The technology also has air purification potential, since it can degrade volatile organic pollutants and nitrogen oxides when included into building materials or air filtration systems (Hernández-Alonso et al., 2009).

Furthermore, photocatalytic disinfection is a chemical-free method of water purification that successfully inactivates pathogens via oxidative damage to biological structures (Murgolo et al., 2019).

Photocatalytic energy applications offer intriguing opportunities for sustainable development, particularly in solar hydrogen production via water splitting and carbon dioxide reduction to useful fuels (Wang et al., 2009; Ohtani, 2010). These processes use abundant solar energy to address key energy needs while mitigating climate change effects. Recent research has focused on increasing efficiency through advanced material design, such as Z-scheme systems and co-catalyst development, as well as investigating low-cost alternatives appropriate for a variety of geographical and economic circumstances (Schneider et al., 2014; Adeniji et al., 2020).

Despite these advancements, scaling up photocatalytic technology presents various hurdles that necessitate ongoing study and innovation. Limitations in quantum efficiency due to charge recombination, catalyst deactivation in real-world settings, and the necessity for improved reactor designs remain major barriers to wider application (Pera-Titus et al., 2004). The future of photocatalysis lies in the development of integrated systems that incorporate various technologies and are suited to specific environmental and energy applications. For regions such as Africa, solar-driven photocatalysis tailored to local conditions and waste streams provides particularly promising solutions to pressing water and energy concerns, indicating the technology's potential to significantly contribute to global sustainable development goals.

Photocatalysis has developed as an important solution for dealing with the environmental problems caused by cassava processing wastewater, which contains high levels of cyanide compounds, organic matter, and other hazardous elements. Traditional treatment methods frequently fail to fully detoxify this complex effluent, making photocatalysis especially advantageous due to its

ability to destroy persistent contaminants via advanced oxidation processes (Adewuyi, 2020). The technology's relevance stems from its ability to entirely mineralize cyanide into harmless end products such as carbonates and nitrogen gas while also lowering the organic load of wastewater under mild reaction conditions (Oluwafemi et al., 2019).

Photocatalytic treatment of cassava wastewater has the benefit of being compatible with solar energy, making it potentially cost-effective for small-scale processors in tropical regions with high cassava output (Boakye et al., 2019). Unlike biological treatment approaches, which can be stopped by cyanide toxicity, photocatalysis is effective throughout a wide range of pollutant concentration. Research in Nigeria and Ghana has shown that modified titanium dioxide photocatalysts can remove over 90% of cyanide from cassava wastewater within hours of solar irradiation (Adeniji et al., 2020; Tichapondwa et al., 2021). The technique also effectively eliminates the characteristic odor and color of wastewater while inactivating pathogenic bacteria, addressing numerous pollution factors at once.

The environmental benefits of photocatalytic treatment are in line with the cassava industry's sustainable development goals. By converting harmful cyanide compounds into innocuous molecules and lowering the organic load that depletes oxygen in bodies of water, the method protects aquatic ecosystems and downstream water consumers. Furthermore, the solar-powered nature of the process lowers energy expenses and carbon footprint when compared to traditional treatment methods. As African countries strive to modernize their cassava processing industries, photocatalysis presents a possible answer to the long-standing difficulty of wastewater management, while also promoting the industry's environmental sustainability and compliance with increasingly stringent regulations.

Hence, this research is driven by the necessity to create a treatment method for cassava wastewater that is both low-cost and highly efficient, utilizing the combined effects of adsorption and photocatalysis in an acid-activated clay-TiO_2 composite when exposed to UV light

STATEMENT OF PROBLEM

Although the cassava processing industry is crucial for the economy, it produces large quantities of wastewater that causes significant pollution. This creates two interconnected issues: environmental damage and threats to public health. Due to its elevated organic load, the direct discharge of this effluent poses a serious risk to aquatic ecosystems by causing severe oxygen depletion in water bodies, resulting in eutrophication and the demise of aquatic fauna (Adelekan et al., 2021). Moreover, the occurrence of cyanogenic glycoside compounds that decompose into the poisonous hydrogen cyanide delivers a powerful toxin to the ecosystem. This contaminates groundwater and surface water utilized for drinking and irrigation purposes, thus posing a threat to public health (Okafor et al., 2022).

Traditional methods of treating wastewater have shown to be insufficient for meeting this challenge, especially for the mainstay small- and medium-scale processors in the industry. Although biological treatment systems like anaerobic digesters are widely used, they frequently suffer from inefficiency stemming from factors such as the seasonality of processing, the requirement for expert operation, and cyanide's detrimental impact on microbial consortia. These issues contribute to unstable performance (Adewuyi & Ogunlaja, 2020). Moreover, the significant capital and operational expenses linked to advanced treatment technologies make them excessively costly and impractical for large-scale implementation (Olojede et al., 2023).

This crucial gap highlights the urgent necessity to create an effective treatment technology that is inexpensive and ecologically sustainable. A technology like this has to be able to efficiently break

down complex organic pollutants and neutralize cyanide in cassava wastewater without producing secondary waste or depending too much on complicated infrastructure. By creating a photocatalytic system that incorporates locally available materials such as clay and a strong oxidant like TiO_2, we can develop an effective and cost-efficient decentralized treatment solution for this ongoing issue.

AIM AND OBJECTIVE OF THE STUDY

This project aims to evaluate the efficiency of acid-activated clay-TiO_2 composites in the photocatalytic degradation of cassava wastewater under UV light and create a cost-effective photocatalytic system using activated clay-supported titanium dioxide (TiO_2) to completely degrade hazardous contaminants in cassava processing.

The objectives of this study are:

i. To characterize the raw clay mineral and to prepare acid-activated clay.

ii. To synthesize and characterize acid-activated clay and titanium dioxide photocatalyst using techniques such as Scanning Electron Microscopy (SEM), X-ray Diffraction (XRD), Fourier Transform Infrared Spectroscopy and X-Ray Fluorescence (XRF).

iii. To assess the composite material's photocatalytic effectiveness in degrading cyanide compounds and organic contaminants with a photocatalytic reactor under UV light.

iv. To evaluate the photodegradation efficiency of cyanide removal in cassava wastewater under varying conditions such as pH, catalyst dosage, irradiation time and wastewater concentration using acid-activated clay-TiO2 composites.

v. To assess the photocatalytic activity of the synthesized composites for the degradation of cassava wastewater.

vi. To determine the kinetics of the photocatalytic degradation process.

SCOPE OF THE STUDY

This project is a laboratory scale study carried out at the chemical engineering laboratory of the university of Benin, Benin City. The clay sample (kaoline and bentonite) used was gotten from Auchi in Edo state, Nigeria prepared by acid activation in the school laboratory and the Cassava wastewater sample used was obtained from a local cassava processing unit. It focuses on the photodegradation of cassava wastewater using activated clay and TiO_2 as photocatalysts under UV light irradiation. This study will measure degradation efficiency through parameters such as COD, BOD and cyanide removal and the pH of the wastewater while investigating key parameters such as pH, catalyst dosage and irradiation time and concentration of wastewater.

Photocatalysts will be characterized using SEM, XRD, FTIR, and XRF studies to better understand their structural and surface properties.

SIGNIFICANCE OF THE STUDY

This research is highly promising for both applied environmental technology and basic science. Its main goal is to create a photocatalyst that is inexpensive and sourced locally by using natural clay as a support for TiO_2. This could render advanced wastewater treatment more feasible from an economic standpoint, particularly for small-scale industries in developing areas (Olad et al., 2020). This research provides an effective approach to reducing the high organic load and toxic cyanide levels in cassava wastewater, offering a direct and sustainable solution to a significant environmental pollution problem. This contributes to cleaner production practices in the agro-processing industry and helps safeguard aquatic ecosystems (Adewuyi & Ogunlaja, 2020).

This work will provide valuable insights into composite photocatalysts and Advanced Oxidation Processes (AOPs) from a scientific perspective, especially by clarifying the synergistic mechanism linking the adsorptive properties of acid-activated clay with the photocatalytic activity of TiO_2

(Djellabi et al., 2019). In addition, the technology and core principles set forth here could be applied more widely, as they might be tailored to address other difficult agro-industrial effluents with comparable traits, such as those produced by palm oil or distillery processes. This would expand the influence of this research beyond just one industrial domain (Aragaw & Alene, 2022).

CHAPTER 2

LITERATURE REVIEW

2.1 CASSAVA WASTEWATER: COMPOSITION AND ENVIRONMENTAL IMPACT

Cassava (Manihot esculenta Crantz), a vital tropical staple crop cultivated in numerous regions around the world, is primarily valued for its starchy roots. These roots serve as the raw material for a diverse array of food products and industrial applications. Among the popular food products derived from cassava roots are tapioca, a widely used thickening agent and dessert ingredient, garri, a granular flour commonly consumed in West Africa, and fufu, a dough-like staple food also prevalent in West Africa. Furthermore, cassava roots are an important source of industrial starch, which finds application in various manufacturing processes (FAO, 2022).

Fig.2.1: Cassava

Cassava processing, involving steps such as washing, peeling, and pressing, inevitably generates substantial quantities of wastewater. This wastewater is known by different names depending on the region, being called "manipueira" in Brazil and "cassava mill effluent" in many parts of Africa, as noted by Cereda & Vilpoux (2019). The volume of wastewater produced is considerable; for every ton of cassava that is processed, approximately 1,000 to 1,500 liters of wastewater are generated. This significant volume presents a challenge, as the wastewater, if not properly treated

and managed, can become a major source of environmental contamination, a concern highlighted by Aworanti et al. (2020).

Indeed, the large volumes of highly polluted wastewater resulting from cassava processing represent one of the most critical agro-industrial pollution issues confronting many tropical nations. The effluent discharged from cassava processing plants has detrimental effects on ecosystems. This is due to its complex composition, which includes cyanogenic compounds capable of releasing poisonous cyanide, fermentable organic waste that consumes oxygen as it decomposes, acidic byproducts that can alter the pH of the environment, and suspended particles that can reduce water clarity and smother aquatic habitats. Consequently, cassava wastewater presents a multifaceted environmental hazard. Unlike many other types of agro-industrial waste, the danger posed by cassava wastewater is both immediate and long-lasting. It combines the immediate threat of cyanide toxicity with the longer-term disruption of ecosystems caused by the depletion of oxygen due to the heavy organic load present in the effluent. This persistent environmental risk emphasizes the importance of effective wastewater management strategies in cassava processing.

Fig.2.2: Cassava Processing Plant

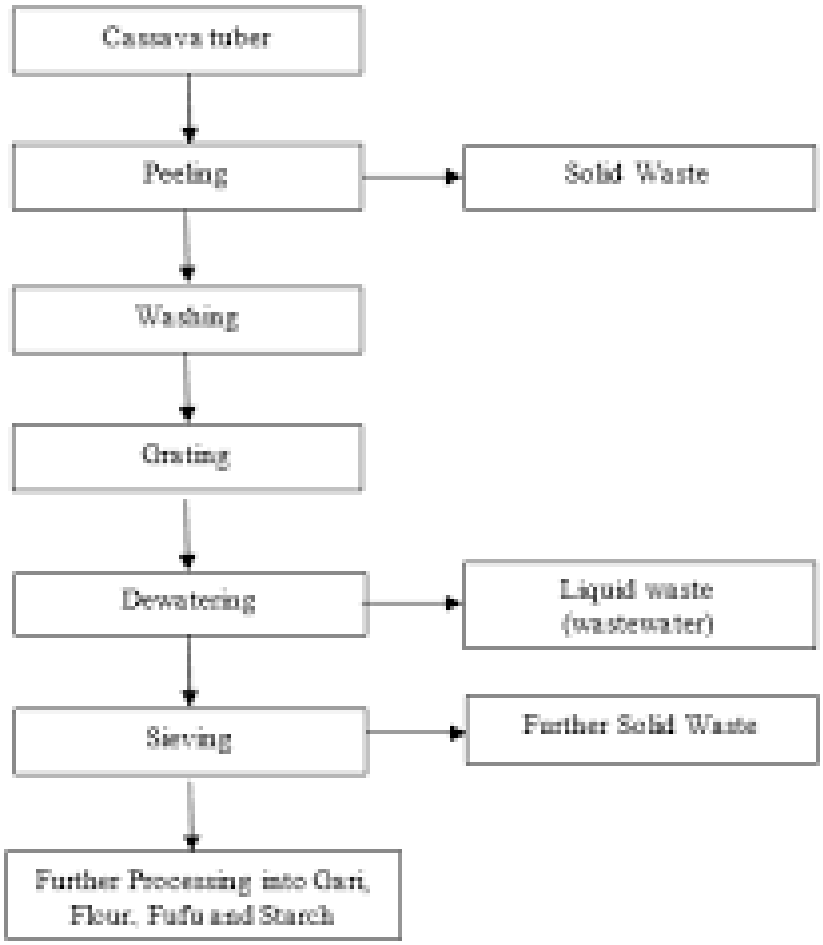

Fig.2.3: Flowchart for Cassava Processing

2.1.1 CASSAVA PROCESSING STEPS THAT GENERATES WASTEWATER

Cassava processing requires multiple important processes that produce significant effluent with a high organic load, cyanide concentration, and suspended particles. The particular wastewater generation sites vary depending on the ultimate product generated, such as garri, flour, starch, or tapioca. Understanding these processing processes is critical to establishing efficient wastewater treatment techniques.

a) Peeling and Washing

Cassava processing begins with the removal of the outer bark and peel, which can be done automatically or manually, followed by thorough washing to remove any soil or debris. This

procedure produces wastewater that contains a high concentration of suspended particles from soil and peel residues, as well as organic materials from damaged tubers. Crucially, this procedure generates cyanide leachate when linamarin and lotaustralin (cyanogenic glycosides) breakdown in the wash water. The volume of wastewater produced per ton of processed cassava is between 500 and 1,000 liters, indicating a large waste stream that must be carefully managed.

b) Grating and pulping

After peeling, cassava is grated into a pulp to shatter cells and release starch. This mechanical method produces starch-rich effluent that includes fine cassava particles, organic acids, and soluble sugars. Importantly, the grating process accelerates linamarin's enzymatic hydrolysis by linamarase, which produces hydrogen cyanide that enters the wastewater stream. This procedure typically generates 1,000-1,500 liters of wastewater per ton of cassava, with the effluent comprising both particulate and dissolved organic contaminants that add significantly to the overall organic load.

c) Fermentation Process

For products such as garri, the pulp is fermented for one to five days to produce flavor, reduce cyanide concentration, and facilitate dewatering. This biological process produces fermentation liquor, known locally as manipueira, which is very acidic with pH levels ranging from 4.0 to 5.0. The wastewater comprises organic acids (mostly lactic and acetic acid), ethanol, and residual cyanide chemicals. The high biological and chemical oxygen demand (BOD/COD ranges from 10,000 to 50,000 mg/L) is caused by the release of soluble organics during fermentation. This stage produces around 200-500 liters of effluent per ton of processed cassava.

d) Pressing and Dewatering

Following fermentation, the pulp is pressed to extract surplus water and concentrate starch. This mechanical separation produces press liquor, which mixes with the fermentation fluid and contains soluble sugars, organic acids, and residual cyanide compounds. This stream has a significant pollutant load, with COD levels of up to 60,000 mg/L, making it one of the most concentrated waste streams in cassava processing. The volume of wastewater produced during this stage normally ranges between 300 and 700 liters per ton of cassava.

e) Starch Extraction and Washing

In cassava processing, separating starch from fibrous pulp via sedimentation, centrifugation, or screening generates a significant amount of wastewater. This process yields starch whey containing fine starch particles, proteins, and soluble cyanide at quantities ranging from 50 to 200 mg/L (as HCN equivalent). The volume of wastewater generated at this stage is significant, averaging 2,000-3,000 liters per ton of cassava, making it the largest contributor to overall wastewater volume in processing plants.

f) Drying and Finishing Operations

The last manufacturing procedure entails drying wet starch or cake to reduce moisture content to levels suitable for storage and distribution. While this procedure produces less effluent than previous stages, the floor washdown water contains residual starch and organic matter, which adds to the overall pollution burden. Despite its low volume, this wastewater stream requires control due to its concentrated character.

2.1.2 CHEMICAL COMPOSITION OF CASSAVA WASTEWATER

Cassava wastewater, also known as manipueira, is a byproduct generated from the processing of cassava roots (Manihot esculenta) into various products such as flour, starch, and fermented foods.

The precise chemical composition of this wastewater is subject to variability, influenced by several key factors including the specific processing techniques employed, the particular variety of cassava being utilized, and the specific conditions under which fermentation occurs, if applicable. Among the important chemical compounds present in cassava wastewater are cyanogenic glycosides, notably lotaustralin and linamarin. These compounds are significant due to their potential to release toxic hydrogen cyanide (HCN) when acted upon by enzymes within the digestive system. The concentration of these cyanogenic glycosides can vary, but typically falls within a range of 50 to 500 milligrams of HCN equivalents per liter, as reported by Cardoso et al. in 2005. In addition to cyanogenic glycosides, cassava wastewater also contains carbohydrates. These carbohydrates, which include sucrose, glucose, and residual starch, are present as a consequence of incomplete or insufficient starch breakdown during the cassava processing. Furthermore, the natural fermentation processes that may occur during cassava processing lead to the formation of various organic acids. While small amounts of acetic, formic, and succinic acids may be produced, lactic acid is often the predominant organic acid present, alongside a broader spectrum of other organic acids, as documented by Okafor et al. in 2007. The presence and concentration of these various components collectively define the overall characteristics of cassava wastewater.

Cassava wastewater which is released during processing of cassava can have potentially harmful effects on the environment typically due to its high organic load and toxic chemical components. Cassava wastewater is a complex effluent containing:

I. Cyanogenic Glycosides and Free Cyanide

The cyanide content in cassava wastewater warrants special consideration due to its severe toxicity and persistence in the environment. When cassava roots are crushed during processing, the cellular disturbance brings linamarin, cassava's principal cyanogenic glycoside, into contact with the

enzyme linamarase, triggering a metabolic cascade that releases hydrogen cyanide (HCN) (Nharingo et al., 2015).

Generally, cyanide concentrations range from 50–500 mg/L in raw effluent, far exceeding the WHO permissible limit of 0.1 mg/L for drinking water (Okafor et al., 2021). Cyanide exists in wastewater in both free and complexed forms, with complexed cyanides having more environmental persistence because they gradually degrade into free cyanide over time. Cyanide pollution leads to acute toxicity in aquatic ecosystems, inhibiting cytochrome oxidase and causing fish kills (Kuyucak & Akcil, 2013) and chronic human exposure causes neurotoxicity, goiter, and konzo (a paralytic disease) (Banea et al., 2017).

II. High Organic Load

While cyanide is the most hazardous component, the organic load in cassava wastewater causes a different but equally harmful type of environmental damage. The effluent often contains fermentable sugars and starches and the high organic content results from these soluble starch, proteins, and fermentable sugars, promoting microbial growth that depletes oxygen in water bodies (Achinas et al., 2020) resulting in BOD values ranging from 8,000 to 20,000 mg/L (Oboh & Aluyor, 2009) and Chemical Oxygen Demand (COD) ranging from 10,000–25,000 mg/L (Nwabanne & Onukwuli, 2012) which is approximately 400 times greater than raw home sewage. When released into rivers or streams, this organic overload causes large microbial blooms that deplete dissolved oxygen, resulting in anoxic dead zones that cannot support most aquatic life. The breakdown process produces foul-smelling gases such as hydrogen sulfide and methane, while the acidic pH (usually 4.0-5.5) dissolves metal ions from sediments, enhancing heavy metal mobility in water systems. Long-term discharge sites exhibit catastrophic benthic ecosystem

collapse, including the loss of macroinvertebrate populations and switches to anaerobic microbial communities.

Cassava wastewater, with its high organic content, has potential applications in biogas production, bioethanol fermentation, and organic fertilizer following cyanide detoxification (Balagopalan, 2002). However, its toxicity requires thorough treatment before disposal or reuse.

III. Acidity and Other Pollutants

Cassava wastewater is extremely acidic, with a pH range of 4.0-6.0, due to the buildup of organic acids (Oluwasola et al., 2021). Its high biological oxygen demand and chemical oxygen demand make it a major environmental contaminant if released untreated (Ubalua, 2007).

Additionally, remaining peel matter may include trace levels of phenolic chemicals, such as tannins. It also concatins phosphates, nitrates and heavy metals (e.g, iron, zinc) from processing equipments (Ubalua, 2019). Lactic acid bacteria and yeasts are among the microorganisms present, which contribute to spontaneous fermentation.

2.1.3 ENVIRONMENTAL IMPACTS OF CASSAVA WASTEWATER

Cyanide toxicity mixed with organic pollutants causes long-term environmental damage. Soil systems that receive cassava wastewater show conventional symptoms of ecological degradation, including acidification to pH levels below 4.0, disruption of mycorrhizal networks, and near-total loss of earthworm populations. Cyanide residues impede nitrification processes, interrupting nitrogen cycle and lowering soil fertility. Perhaps most concerning is the bioaccumulation potential; studies in the Niger Delta have found cyanide concentrations in edible plants growing in wastewater-contaminated soils that surpass 15 mg/kg, posing direct dangers to human health

throughout the food chain. Some of the environmental impacts of untreated cassava wastewater includes:

I. . Water Pollution**:** When discharged untreated, cassava wastewater causes eutrophication due to nutrient overload (Nwoko & Ogunyemi, 2018) and Cyanide contamination renders water unsafe for drinking and irrigation (Nharingo et al., 2015). Oxygen depletion from microbial decomposition of organic matter leads to fish kills and loss of aquatic biodiversity (Achinas et al., 2020).

II. Soil Degradation: Acidic pH and cyanide inhibit soil microbial activity**,** reducing fertility (Okafor, 2018). Long-term discharge of cassava wastewater results in heavy metal accumulation, affecting crop growth (Ubalua, 2019).

III. Air Pollution: Decomposing organic matter releases methane (CH_4) and hydrogen sulfide (H_2S)**,** contributing to greenhouse gas emissions (FAO, 2022).

When examining production volumes, the scope of this environmental catastrophe becomes clear. During peak processing seasons, Nigeria alone produces an estimated 50 million liters of cassava wastewater every day. With less than 5% of small-scale processors using any form of treatment, the cumulative impact is one of the most significant unregulated pollution sources in tropical agriculture. The persistence of cyanide in anaerobic sediments, its bioaccumulation potential, and its synergistic effects with other wastewater components present an environmental management challenge that necessitates immediate attention and novel solutions, such as the photocatalytic degradation methods investigated in this study.

2.2 CONVENTIONAL AND ADVANCED TREATMENT METHODS FOR CASSAVA WASTEWATER

Cassava wastewater treatment poses a daunting challenge due to its complicated composition, which includes high cyanide content, severe organic loading, and acidic pH levels. Various treatment procedures, ranging from simple ancient methods to sophisticated modern technologies, have been tried with various degrees of effectiveness. Effective treatment is required to reduce environmental damage and promote resource recovery. Wastewater treatment technologies can be roughly classified into physical, chemical, and biological procedures, each with unique benefits and drawbacks in cassava wastewater management. This section thoroughly examines various technologies, assessing their efficacy, limitations, and relevance to cassava wastewater treatment, while emphasizing the critical need for more sustainable and efficient alternatives.

PHYSICAL TREATMENT METHODS

Physical treatment is the process of removing impurities via mechanical or physical separation while preserving their chemical composition.

Common techniques include:

a. **SEDIMENTATION AND DECANTATION:** Sedimentation and decantation are two of the most basic processes for separating particles from liquids, using gravity settling and porous media. However, these approaches are mainly unsuccessful for cassava wastewater because to the high concentration of dissolved contaminants, particularly cyanide and soluble organic compounds (Okafor et al., 2021).

Advantages:

i. It is simple and inexpensive (Ubalua, 2007).
ii. It is effective for removing coarse particle materials (such as starch residues).

Disadvantages:

i. It does not remove dissolved contaminants such as cyanide and organic acids.
ii. Large areas of land are required for settling ponds.

b. **MEMBRANE FILTRATION:** Membrane and sand filtration involves passing wastewater through porous media such as sand, activated carbon, or synthetic membranes. Membrane filtration, which includes ultrafiltration (UF) and reverse osmosis (RO), has showed promise for eliminating both suspended and dissolved pollutants. Nwabanne and Onukwuli (2019) found 85-90% cyanide rejection with nanofiltration membranes. However, membrane fouling, high operating costs, and energy requirements make this technique unsuitable for small-scale cassava processors in impoverished countries.

Advantages:

i. It removes fine suspended particles and some organic debris (Okafor et al., 2007).
ii. It can be used with other treatment methods to increase efficiency.

Disadvantages:

i. Membrane fouling drives up maintenance expenses (Balagopalan, 2002).
ii. It is ineffective against dissolved cyanide and chemical compounds with a low molecular weight.

c. **EVAPORATION AND SOLAR DRYING:** Water evaporates, resulting in concentrated sludge.

Advantages:

i. This method reduces wastewater volume (Nambisan 2011).

ii. It Can recover nutrients for use in fertilizer.

Disadvantages:

i. It is Slow and weather dependent.

ii. It does not breakdown cyanide or organic contaminants.

Another physical-chemical strategy is coagulation-flocculation, which uses coagulants (such as alum and ferric chloride) to aggregate tiny particles into bigger flocs that may be removed by sedimentation. Aworanti et al. (2017) found that polyaluminum chloride (PACl) might reduce COD in cassava wastewater by up to 60%; however, this method fails to address cyanide toxicity and needs huge amounts of chemicals, resulting in hazardous sludge.

CHEMICAL TREATMENT METHODS

Chemical treatment methods are particularly valuable for cassava wastewater due to their ability to rapidly degrade or transform hazardous compounds. Pollutants are often neutralized through oxidation, precipitation, or pH modification. Chemical treatment strategies use reagents to neutralize, oxidize, or precipitate contaminants. Alkaline chlorination is a popular cyanide detoxification process that involves raising the pH over 10 and adding chlorine to convert cyanide into less harmful cyanate. Kuyucak and Akcil (2013) found that this approach removed more than 95% of cyanide, although the generation of hazardous chlorinated byproducts (such as cyanogen chloride) and high chlorine consumption restrict its long-term viability.

Advanced Oxidation Processes (AOPs), including Fenton's reagent (Fe^{2+}/H_2O_2) and ozonation, produce hydroxyl radicals (•OH) that break down organic contaminants and cyanide. Oluwasola et al. (2021) reduced COD by 80% using Fenton oxidation, however the acidic pH requirement (pH 2-4) is incompatible with the natural acidity of cassava effluent, demanding further pH adjustment. Furthermore, sludge formation and residual iron contamination are unresolved issues. These Chemical processes includes:

a. **CYANIDE DETOXIFICATION:** Cyanide detoxification is one of chemical treatment's most critical applications. Cassava wastewater contains linamarin and lotaustralin, which hydrolyze to produce hydrogen cyanide (HCN), a powerful poison. Alkaline chlorination involves reacting sodium hypochlorite (NaOCl) with cyanide in an alkaline medium (pH > 10) to produce cyanate (OCN^-), a less hazardous compound. Alkaline chlorination (NaOCl + NaOH) transforms cyanide into less harmful cyanate (Cardoso et al., 2005). This reaction happens in two steps: first, cyanide is oxidized to cyanogen chloride (CNCl), which is then hydrolyzed to cyanate in the presence of excess alkali (Cardoso et al., 2005). While effective, this approach has downsides, including the generation of chlorinated byproducts, which may require further treatment.

Hydrogen peroxide (H_2O_2) oxidation is a safer alternative to chlorination since it does not produce toxic chlorine compounds. Hydrogen peroxide interacts with cyanide in alkaline circumstances to form cyanate, which then decomposes into carbon dioxide and nitrogen. The reaction is effective, but it requires careful pH control and enough peroxide dosage to remove all cyanide (Ahaotu et al., 2013). One advantage of peroxide treatment is that it does not produce new hazardous residues, making it more environmentally friendly. However, the expense of hydrogen peroxide can be prohibitively expensive in large-scale applications.

Advantages:

i. Cyanide can be removed quickly and effectively (with above 95% efficiency).

ii. It is Suitable for cyanide-rich wastewater (Ahaotu et al., 2013).

Disadvantages:

i. High chemical expenses.

ii. Produces hazardous byproducts (such as chlorinated chemicals).

b. **COAGULATION-FLOCCULATION (Alum, Ferric Chloride, or Natural Coagulants):** Coagulation-flocculation is another chemical process used to treat cassava wastewater, primarily to remove suspended particles and colloidal organic debris. Aluminium sulfate (alum), ferric chloride, and polyaluminum chloride (PAC) are common coagulants. These compounds neutralize the charges of suspended particles, leading them to collect into bigger flocs that may be removed via sedimentation or filtration. Natural coagulants, such as Moringa oleifera seed extract, have also been studied as environmentally friendly alternatives (Ubalua, 2007). Coagulation enhances effluent clarity, but it does not eliminate dissolved cyanide or low-molecular-weight organic contaminants, needing additional treatments.

Advantages:

i. Reduces turbidity and organic load (UBalua, 2007).

ii. It can be combined with sedimentation.

Disadvantages:

i. Sludge formation necessitates disposal.

ii. It does not decompose cyanide.

c. **NEUTRALIZATION (pH adjustment using lime or alkali):** pH adjustment is an important chemical treatment step for cassava wastewater, which is normally acidic (pH 4.0-6.0). To neutralize acidity before biological treatment, lime ($Ca(OH)_2$) or sodium hydroxide (NaOH) is commonly used, as many bacteria require pH values close to neutral. Neutralization also helps to precipitate some metal ions, lowering their solubility. However, this process does not degrade organic pollutants and may produce sludge that needs to be disposed of.

Advantages:

Reduces acidity, making wastewater suitable for disposal or further treatment.

Disadvantages:

i. it Does not eliminate organic contaminants.

ii. Excessive chemical usage.

Another chemical treatment method is Sulfite-assisted oxidation involves using sulfur dioxide (SO_2) or sodium metabisulfite ($Na_2S_2O_5$) with a copper catalyst to convert cyanide to thiocyanate (SCN^-). While thiocyanate is less hazardous than free cyanide, it still requires extra treatment before being dumped into water bodies. This approach is less typically utilized for cassava wastewater, although it could be useful in industrial settings where sulfur-based compounds are easily available.

Additionally, Electrochemical therapy, particularly electrocoagulation (EC), has grown in popularity due to its ability to remove organics, cyanide, and heavy metals all at once. Ubalua (2019) demonstrated 75-90% cyanide decomposition using aluminum electrodes, but energy costs and electrode passivation limit scalability.

INTEGRATION OF OTHER TREATMENT METHODS

Given these constraints, chemical treatments are frequently paired with biological processes to create a more sustainable solution. For example, cyanide can be chemically oxidized to lessen toxicity before being degraded via anaerobic digestion. Alternatively, coagulation can be employed to remove solids prior to biological treatment. These hybrid systems maximize efficiency while reducing chemical consumption and operating expenses.

BIOLOGICAL TREATMENT METHODS

Biological processes use microorganisms to degrade organic contaminants and detoxify cyanide. Aerobic treatment, such as activated sludge systems, can reduce BOD by 70–85% (Achinas et al., 2020). However, the high cyanide level limits microbial activity, necessitating prolonged acclimation times.

Anaerobic digestion is better suited to high-strength wastewater, producing biogas (methane) as a useful byproduct. Cereda and Vilpoux (2019) demonstrated a 90% reduction in organic load in Brazilian cassava plants utilizing up flow anaerobic sludge blanket (UASB) reactors. However, cyanide toxicity to methanogens and lengthy beginning durations (6-8 weeks) prevent widespread adoption.

Constructed wetlands, a low-cost alternative, use phytoremediation to eliminate contaminants. Nharingo et al. (2015) found that Typha latifolia (cattail) removed 60-70% of cyanide in Zimbabwe.

EMERGING AND HYBRID TREATMENT TECHNOLOGIES

ADVANCED OXIDATION PROCESSES (AOPS).

Advanced Oxidation Processes (AOPs) consist of various chemical treatment methods aimed at eliminating organic and inorganic contaminants in water and wastewater via oxidation reactions

involving hydroxyl radicals (•OH). These radicals are potent, non-selective oxidants with an electrochemical oxidation potential of 2.8 V, surpassed only by fluorine (Miklos et al., 2018). AOPs are characterized by the in-situ production of •OH radicals in adequate amounts to treat wastewater effectively. Through primary mechanisms like radical addition, hydrogen abstraction, electron transfer, and radical combination, these radicals engage with organic pollutants. This process culminates in the mineralization of contaminants into carbon dioxide, water, and inorganic ions (Andreozzi et al., 1999).

AOPs can be classified broadly according to how hydroxyl radicals are generated. Homogeneous AOPs, where the catalyst shares the same phase as the wastewater, encompass methods such as ozonation—where ozone breaks down in water to produce •OH radicals—and the Fenton process, which employs a combination of ferrous ions and hydrogen peroxide to create •OH radicals in an acidic environment. On the other hand, heterogeneous AOPs utilize a catalyst that is usually a solid and exists in a different phase than the wastewater. The most notable instance is heterogeneous photocatalysis, which utilizes a semiconductor catalyst that forms electron-hole pairs when irradiated with light of adequate energy. These pairs subsequently interact with water and oxygen to generate reactive oxygen species, such as •OH radicals (Chong et al., 2010). This process is particularly attractive because it can utilize solar energy and the catalyst can be reused.

AOPs offer a notable benefit for the treatment of cassava wastewater. Not only can they diminish the elevated levels of chemical oxygen demand, but they can also entirely eliminate complex cyanide molecules, transforming them into products that are less harmful, such as cyanate, carbonates, and nitrogen gas. This is something that traditional biological methods cannot do efficiently (Oluwafemi et al., 2019). Due to their non-selectivity, •OH radicals can simultaneously

degrade a broad range of organic pollutants. This makes advanced oxidation processes (AOPs) such as heterogeneous photocatalysis a highly promising and essential technology for this research. Given the limits of traditional approaches, researchers are investigating integrated systems that combine physicochemical and biological processes. Photocatalysis, employing TiO_2 and activated clay, is a sustainable approach that uses solar energy to degrade pollutants. Okafor et al. (2022) found that under optimal circumstances, >90% of cyanide could be removed with minimum sludge generation.

Microbial fuel cells (MFCs) are another novel technique in which electroactive bacteria breakdown organics while producing power. Ezemonye and Ogbomida (2019) accomplished simultaneous COD reduction and bioenergy recovery, although cyanide inhibition remains a challenge.

Table.2.1Comparative Analysis for Cassava Wastewater Treatment:

Method	**Advantages**	**Disadvantages**	**Suitability for Cassava Wastewater**
Sedimentation	Low-cost, simple	Does not remove dissolved pollutants	Preliminary treatment only
Chemical Oxidation	Fast cyanide removal	Expensive, toxic byproducts	Critical for high-cyanide wastewater
Anaerobic Digestion	Energy recovery, high BOD removal	Slow, sensitive to pH	Best for large-scale treatment
Aerobic Treatment	Effective BOD reduction	High energy demand	Secondary treatment after cyanide removal

2.3. PHOTOCATALYSIS: PRINCIPLES AND MECHANISM

2.3.1 INTRODUCTION TO PHOTOCATALYSIS

Photocatalysis is an advanced oxidation process (AOP) that uses light energy to speed up chemical reactions in the presence of a catalyst. This technique has received a lot of interest in environmental remediation, especially for wastewater treatment, because of its capacity to breakdown organic contaminants, inactivate microorganisms, and even detoxify dangerous chemicals like cyanide found in cassava wastewater (Fujishima & Honda, 1972). Photocatalysis, unlike traditional treatment methods, works under mild conditions (ambient temperature and pressure) and can completely mineralize contaminants into innocuous byproducts like CO_2 and H_2O (Hoffmann et al., 1995). Traditional treatment procedures frequently fail to fully mineralize these contaminants, but photocatalysis has the potential for total breakdown into harmless end products (Li et al., 2015). Photocatalytic devices are adaptable to a wide range of scales, from small decentralized units to big industrial treatment plants, with the added benefit of solar-powered operation (Malato et al., 2009).

2.3.2 FUNDAMENTAL PRINCIPLES OF PHOTOCATALYSIS

Photocatalysis activates semiconductor materials (e.g., TiO_2, ZnO, or g-C_3N_4) by photons with energy equal to or greater than their bandgap. When illuminated, electrons (e^-) in the valence band (VB) are excited to the conduction band (CB), leaving behind positively charged holes (h^+) that drive redox reactions that decompose pollutants (Linsebigler et al., 1995). It involves the acceleration of a photoreaction in the presence of a catalyst, typically a semiconductor material which absorbs light to generate reactive species for chemical transformations. It relies on light energy (usually UV or visible light) to initiate these reactions often in atmospheric conditions, making is energy-efficient and environmental friendly.

$$\textbf{Photocatalyst} + h\nu \rightarrow e^{-}_{CB} + h^{+}_{VB}$$

COMPONENTS OF PHOTOCATALYSIS

I. Semiconductor Catalyst: This is the material that absorbs light to generate electron-hole pairs, which facilitates redox reactions without being consumed. The most widely used photocatalyst is titanium dioxide (TiO_2) due to its chemical stability, non-toxicity, and high photocatalytic activity (Fujishima et al., 2008). Other catalyst includes, Zinc oxide (ZnO). ZnO has a bandgap similar to TiO_2(3.37 eV) and exhibits strong photocatalytic performance, but is susceptible to photocorrosion in aqueous conditions (Zhang et al., 2014), Graphitic carbon nitride (g-C3N4) Ong et al. (2016) discovered a metal-free polymer semiconductor with a bandgap of around 2.7 eV that is chemically stable and shows visible light activity, etc.

II. Light Source: This provides the energy to excite electrons in the photocatalyst, typically UV, visible or near-infrared light depending on the catalyst bandgap. UV light ($\lambda < 387$ nm for TiO_2) is commonly utilized, however visible-light-activated catalysts are being developed for solar-powered applications (Asahi et al., 2001).

III. Substrate/Reactants: These are molecules that undergo oxidation or reduction on the catalyst surface.

Oxidizing agents like oxygen (O_2) and hydrogen peroxide (H_2O_2) improve photocatalytic effectiveness by trapping electrons and preventing recombination (Pelaez et al., 2012).

IV. Reaction Medium: That aqueous or gaseous environments where the photocatalytic reaction takes place.

TYPES OF PHOTOCATALYSIS

There are two types of photocatalysis namely:

i. Homogenous photocatalysis: In this type of photocatalysis, the catalyst and reactants are in the same phase for example, dissolved metals in solution. This types of photocatalysis is less common due to challenges in catalyst recovery.

ii. Heterogenous photocatalysis: The catalyst is a solid (e.g., TiO_2 nanoparticles) and the reactants are in a different phase (liquid or gas). This is the most widely studied form of photocatalysis due to easy catalyst separation and its reusability. Semiconductor materials such as titanium dioxide (TiO_2) are employed in heterogeneous photocatalysis to break down organic contaminants upon exposure to light. The process initiates when photons with energy greater than the semiconductor's bandgap excite electrons from the valence band to the conduction band, resulting in the formation of electron-hole pairs (e^-/h^+).

iii. These charge carriers move to the catalyst surface, where they facilitate redox reactions. The hole (h^+) oxidizes water or hydroxide ions to produce hydroxyl radicals (•OH), whereas the electron (e^-) reduces oxygen, resulting in superoxide radicals ($•O_2^-$). These oxygen species, which exhibit a high degree of reactivity—most notably •OH—launch non-discriminatory assaults on organic contaminants via oxidation. This process ultimately leads to their mineralization into innocuous byproducts such as CO_2 and H_2O. This mechanism effectively eliminates both organic load and toxic cyanide compounds in cassava wastewater.

2.3.3 MECHANISM OF PHOTOCATALYSIS

The photocatalytic process can be broken down into several steps namely:

I. **Light Absorption and Charge Generation:** The photocatalytic process begins when a semiconductor absorbs photons with energy (hv) that equals or exceeds its bandgap energy (Eg). When a photocatalyst such as titanium dioxide (TiO_2) absorbs photons with energy equal to or greater than its band gap (3.2 eV for anatase TiO_2), electrons (e^-) are promoted from the valence band to the conduction band, leaving positively charged holes (h^+) in the valence band (Schneider et al., 2023). This excitation can be expressed as:

$$\text{Photocatalyst} + h\nu \rightarrow eCB^- + hVB^+$$

The efficiency of this process is dependent on various factors:

i. Light penetration depth: This is determined by the absorption coefficient of the substance.

ii. Charge separation: Charge separation is influenced by crystal defects and electric fields at interfaces. Strategies for improving charge separation includes Crystal facet engineering to generate internal electric fields or Heterojunction construction for charge transfer.

iii. Recombination rates: these are affected by surface conditions and trapping sites.

Photogenerated charge carriers have short lifetimes (usually nanoseconds to microseconds), therefore they must move to the catalyst surface to engage in redox processes before recombining (Kamat, 2007). Strategies for improving charge separation includes Crystal facet engineering to generate internal electric fields or Heterojunction construction for charge transfer.

II. **Surface Redox Reactions:** At the surface, electrons in the CB reduce electron acceptors while holes in the VB oxidize electron donors. Example of these reactions are:

i. Oxidation Reactions by Valence Band Holes:

Direct oxidation of adsorbed pollutants:

$$\text{Pollutant} + h^+ \rightarrow \text{Oxidized intermediates}$$

Water oxidation to generate hydroxyl radicals:

$$h^+ + H2O \rightarrow \bullet OH + H^+$$

ii. Reduction Reactions by Conduction Band Electrons:

Oxygen reduction to form superoxide radicals:

$$e^- + O_2 \rightarrow \bullet O_2^-$$

Proton reduction for hydrogen evolution:

$$2e^- + 2H^+ \rightarrow H_2$$

iii. Secondary Reactive Species Formation:

Hydroxyl radicals (•OH) from peroxide decomposition:

$$\bullet O_2^- + H2O_2 \rightarrow \bullet OH + OH^- + O_2$$

Singlet oxygen ($^1O_2$) generation via energy transfer.

Pollutant degradation pathway

The reactive oxygen species (ROS) attack organic pollutants through multiple mechanisms which includes:

i. Hydrogen Abstraction: OH radicals extract H atoms from C-H bonds which Creates carbon-centered radicals that react further

ii. Electron Transfer: this involves Direct charge transfer to adsorbed molecules and it is Particularly effective for aromatic compounds

iii. Addition Reactions: •OH adds to double bonds or aromatic rings which Leads to hydroxylated intermediates.

III. **Mineralisation and Byproduct Formation:** Complete mineralization turns organic contaminants into CO_2, H_2O, and inorganic ions. However, partial oxidation can produce intermediate intermediates that are potentially more harmful than their parent molecules. For example, phenol degradation can create benzoquinones before the whole ring opens (Mills & Le Hunte, 1997). Advanced analytical techniques such as LC-MS and GC-MS are critical for monitoring these transformation products.

2.3.4 FACTORS AFFECTING PHOTOCATALYTIC EFFICIENCY

i. Bandgap Energy: this determines the required light wavelength. Narrow bandgap materials can use visible light but may be less stable. Doping with metals (Fe, Cu) or non-metals (N, S) narrows the bandgap for visible-light response (Asahi et al., 2001).

ii. Surface Area: High surface area (>50 m^2/g) increases active sites and enhances pollutant adsorption while Acidic surface groups improve organic compound affinity.

iii. Light Source: UV intensity (usually 1–100 mW/cm^2) influences reaction speeds. The light distribution in reactors must be uniform.

iv. Reaction Conditions: pH, temperature and reaction concentration affects kinetics. pH affects surface charge and ROS production. Elevated temperatures (30-80°C) often improve kinetics. Too high temperatures may encourage recombination.

v. Reactor Design Considerations: Slurry reactors provide better mass transfer, but they require catalyst recovery while Immobilized systems allow continuous operation but may be less efficient.

2.3.5 APPLICATIONS OF PHOTOCATALYSIS

Photocatalysis has demonstrated effectiveness for environmental remediation and degradation of organic pollutants into harmless products. It is used for CO_2 reduction, conversion of CO_2 to fuels

like methane or methanol addresses climate change. TiO_2-coated surfaces(glass,tiles) degrade organic dirt under sunlight and can be used in architecture and automotive industries.

Photocatalysis has been effective for pharmaceutical residue elimination and petrochemical wastewater treatment. TiO_2 photocatalysis is effective for water splitting (photocatalytic splitting of water into H_2 and O_2 for clean energy) (Fujishima and Honda, 1972).

$$2H2O \rightarrow 2H_2 + O_2 \text{ (light photocatalyst)}$$

TiO_2 photocatalysis removes methylene blue from wastewater (Houas et al., 2001).

Additionally, photocatalysis can be used for organic synthesis, that is selective oxidation or reduction of organic molecules for fine chemical synthesis, replacing harsh chemical reagents.

2.3.6 CURRENT CHALLENGES AND FUTURES PERSPECTIVE OF PHOTOCATALYSIS

Despite its potential, photocatalysis faces different challenges which includes:

i. Mass Transfer Constraints: Limited pollutant diffusion to catalyst surfaces and Gas-liquid-solid three-phase challenges
ii. Energy Efficiency: UV lamp energy consumption remains high. Due to charge recombination, only a small fraction of absorbed photons leads to reactions.
iii. Catalyst Stability: Long-term performance degradation, that is some materials suffer from photocorrosion, fouling and poisoning issues.
iv. Scalability: Reactor design complexities, high cost and low efficiency hinder large-scale applications.

Emerging solutions to these challenges has been introduced and they are focused on:

i. Developing visible-light-active photocatalysts : Au/TiO_2 shows 98% activity under visible light

ii. Designing heterostructures for better charge separation

iii. Exploring model materials like 2D materials(MoS2) and metal-organic frameworks (MOFs).

iv. Integrating photocatalysis with renewable energy systems for sustainable applications.

In conclusion, Photocatalysis is a versatile and ecologically friendly technology with tremendous potential for addressing global challenges in energy and environmental sustainability including water pollution issues. Its use in cassava wastewater treatment provides a sustainable alternative for cyanide removal and organic load reduction. While obstacles remain in scaling up and improving energy efficiency, recent research in materials science and reactor engineering promises to overcome these constraints. The combination of photocatalysis and conventional treatment technologies offers a compelling approach to sustainable water management in the food processing industry.

2.4 TITANIUM DIOXIDE (TiO_2) AS A PHOTOCATALYST

Titanium dioxide has emerged as one of the most effective photocatalysts for wastewater treatment due to its high chemical stability, nontoxicity, and oxidizing power. UV light ($\lambda \leq 387$ nm for anatase TiO_2) excites electrons from the valence band to the conduction band, resulting in electron-hole pairs that drive redox processes (Fujishima et al., 2008). African researchers at the University of Johannesburg demonstrated that local anatase TiO_2 samples achieved 85% degradation of methylene blue within 120 minutes of sun simulation (Mamba & Mishra, 2016).

Titanium dioxide's photocatalytic activity is due to its various crystalline arrangements, which each have specific electrical and optical properties. Anatase-phase TiO_2 is widely used in research due to its excellent balance of charge carrier mobility and recombination rates. Its tetragonal structure, with distorted TiO_6 octahedra, creates an internal dipole moment that promotes charge

separation. Rutile-phase materials, despite having a narrower band gap, suffer from faster electron-hole recombination. However, recent studies from South Africa's Council for Scientific and Industrial Research (CSIR) have demonstrated improved rutile performance through strategic doping with transition metals commonly found in African mineral deposits, such as vanadium and chromium extracted from Bushveld Complex ores.

The electronic band structure shows a valence band made up predominantly of oxygen 2p orbitals and a conduction band made up of titanium 3d states, with the exact band gap energy ranging from 3.0-3.2 eV depending on the crystalline phase and defect chemistry. The University of Lagos researchers used spectroscopic ellipsometry to establish that Nigerian-sourced ilmenite-derived TiO_2 had similar band structure features to commercial Degussa P25 after suitable processing. The charge carrier dynamics in these materials exhibit mean free pathways of 10-50 nm for electrons and 1-5 nm for holes, as measured by transient absorption spectroscopy at the University of Cape Town's nanophotonics laboratory.

Table 2.2 : Comparative structural parameters of TiO_2 polymorphs

Parameter	Anatase	Rutile	Brookite
Density (g/cm³)	3.89	4.25	4.12
Ti-O bond length	1.934-1.980 Å	1.949-1.980 Å	1.87-2.04 Å
Dielectric const.	48	110	78

2.4.1 PHOTOCATALYTIC MECHANISM OF TITANIUM DIOXIDE

Photon absorption generates electron-hole pairs, which participate in complicated surface redox processes that promote pollutant degradation. The holes oxidize surface hydroxyl groups or water molecules, producing hydroxyl radicals, whereas electrons decrease adsorbed oxygen, forming superoxides. Kenyan researchers at Jomo Kenyatta University of Agriculture and Technology have demonstrated that the surface chemistry of TiO_2 can be tailored for specific African wastewater contaminants by carefully controlling the hydroxyl group density, which varies from 5-15 OH/nm^2 depending on pretreatment methods. These surface groups act as essential reaction centers, with their protonation state significantly impacting photocatalytic effectiveness across the pH ranges found in African industrial effluents.

The redox chemistry occurs via a variety of mechanisms, including direct hole transfer, hydroxyl radical attack, and sequential oxidation processes, which eventually mineralize organic contaminants to carbon dioxide and water. Egyptian scientists at the National Research Centre have developed detailed kinetic models for these processes. They show that the degradation of common African industrial dyes like Congo red follows Langmuir-Hinshelwood kinetics with rate constants varying from 0.05-0.3 min^{-1} depending on catalyst morphology. Meanwhile, researchers at the University of Ghana have identified the unique degradation pathways for cyanide complexes found in cassava processing effluent, exhibiting complete conversion to nitrate ions via intermediate cyanate production.

2.4.2 APPLICATIONS OF TITANIUM DIOXIDE PHOTOCATALYSIS

Implementing TiO_2 photocatalysis in Africa has shown promising outcomes in several applications. Pilot-scale photocatalytic systems in Nigeria and Morocco have successfully decolored and detoxified dyehouse effluents, attaining removal efficiencies of more than 90% for

several azo dyes. Mining enterprises in South Africa and Zambia have employed TiO_2-based treatments for acid mine drainage. This technique successfully oxidizes ferrous iron and allows heavy metal precipitation. Agricultural districts in Kenya and Ethiopia have installed solar photocatalytic systems to remove pesticides from irrigation runoff, solving a key food safety issue. Advancements in catalyst chemistry and reactor design have made TiO_2 photocatalysis more economically viable. Researchers at the University of Lagos created low-temperature manufacturing methods that use locally available precursors, significantly lowering production costs. Simultaneously, engineering teams at the University of Cape Town developed modular reactor systems that can be quickly expanded to meet treatment needs. These improvements have made photocatalytic water treatment more accessible to small-scale companies and rural people throughout the continent.

Table 2.3 Photocatalytic efficiency of various TiO_2 systems

Photocatalyst System	Pollutant Removed	Efficiency	Time	Light Source	Reference
Fe-doped TiO_2 (South Africa)	Methylene blue	92%	3h	Solar	Mamba, 2017
N-TiO_2 (Egypt)	Reactive red dye	95%	2h	Visible	Abdel-Mottaleb, 2019
TiO_2/graphene (Nigeria)	Ciprofloxacin	89%	4h	UV	Adewuyi, 2020
Au/TiO_2 (USA)	Phenol	98%	1h	Visible	Linsebigler et al., 1995
TiO_2 nanotubes (Brazil)	Paracetamol	100%	6h	Solar	Silva,

2.5 CLAY MINERALS

Clay minerals are hydrous aluminosilicates with layered structures that are found naturally and are classified as phyllosilicates. They are abundant, low-cost, and ecologically friendly materials with distinctive physicochemical qualities such as large surface area, cation exchange capacity (CEC), and adsorption capabilities (Bergaya & Lagaly, 2013). Clays have been extensively explored for their structural versatility in applications such as catalysis, environmental remediation, and as supports for photocatalytic materials like titanium dioxide (TiO_2) (Zhou, 2011). It has also been historically used for buildings, pottery, and other artistic purposes.

The primary appeal of clay minerals stems from its layered structure, large surface area, cation exchange capacity, and ability to undergo numerous changes that tailor their properties to specific purposes.

2.5.1 GEOLOGICAL ORIGIN AND FORMATION OF CLAY MINERALS

Clay minerals are formed by a variety of geological processes that take place under specific climatic conditions. Chemical weathering of primary silicates via hydrolysis reactions degrades feldspars and other aluminosilicates in igneous and metamorphic rocks, especially in tropical climates such as the West African shield regions, where intense weathering results in residual clay deposits. Hot, mineral-rich fluids hydrothermally alter volcanic ash and rocks, transforming them into high-purity smectites, as seen in East African Rift Valley systems.

Sedimentary diagenesis processes convert volcanic ash into bentonite deposits, which are often found in Cretaceous sedimentary basins in North Africa, with smectite transforming to illite at deeper depths. In Saharan playa lakes, unique clay minerals such as palygorskite and sepiolite occur naturally through direct precipitation from solution. These various formation paths produce

clay minerals with different structural, chemical, and physical properties, which affect their performance in environmental applications.

2.5.2 CLASSIFICATION AND PROPERTIES OF CLAY

Clay minerals have a distinctive crystalline structure made up of two main building pieces. Silica tetrahedral sheets are made up of silicon atoms and four oxygen atoms in a tetrahedral configuration (SiO_4), generating extended hexagonal networks with shared basal oxygens. Alumina octahedral sheets consist of six hydroxyl groups or oxygens in an octahedral configuration ($Al(OH)_6$ or $Mg(OH)_6$). These structural elements interact to generate various layered configurations that determine clay mineral characteristics.

Clay minerals are broadly classed according to their layered structure and chemical makeup. The most frequent varieties are kaolinite, montmorillonite, illite, and halloysite, each with unique features that affect their efficacy in general applications.

Kaolinite, a 1:1 phyllosilicate with the chemical formula $Al_2Si_2O_5(OH)_4$, is distinguished by its non-expanding layers and poor cation exchange capacity. Its primary component is kaolin and it is sometimes referred to as China clay. Its whiteness, tiny particle size, and good heat stability makes it one of the most widely used type of clay. With 7Å basal spacing, it is found extensively in African deposits like Nigeria's Abeokuta formation and South Africa's Cape Province. Despite restrictions, kaolinite has been used as a TiO_2 support due to its high thermal stability and abundance in various African locales (Diko et al., 2016).

Montmorillonite, a 2:1 phyllosilicate from the smectite group also known as Bentonite is another type a clay mineral with 10-15Å variable spacing, occurring in Moroccan bentonite deposits and Ethiopian volcanic-derived clays. it has excellent swelling properties and high cation exchange capacity, making it ideal for intercalation with TiO_2 nanoparticles. Studies at African research

institutions have shown that locally produced montmorillonite care useful in photocatalytic composites (Olu-Owolabi et al., 2017). It is beneficial for drilling fluids, waterproofing and detoxifying because it expands when exposed to water.

Illite, another 2:1 clay mineral, has qualities midway between kaolinite and montmorillonite with 10Å fixed spacing, forming in potassium-rich diagenetic environments and widespread in Algeria's Paleozoic shales. It is found in sedimentary layers and shale and it is malleable whereas halloysite, with its distinct tubular shape, provides extra benefits for nanoparticle dispersion and pollutant adsorption (Musyoka et al., 2020).

Different physical and chemical properties of clay sets it apart and dictate it suitability and availability for use in various industries and they include, color, particle size, Plasticity, Water absorption, pH variability, thermal resistance amongst others.

2.5.3 MODIFICATION AND ACTIVATION OF CLAY MINERALS FOR PHOTOCATALYSIS

To improve the performance of clay minerals in photocatalytic systems, several activation and modification approaches have been devised. These methods have been researched on and proven to be useful in the modification of clay minerals for photocatalytic activities and they include:

i. **Acid activation**: One of the most frequent procedures is acid activation, which includes treating clay minerals with mineral acids like hydrochloric and sulfuric acid. This method has several benefits: it increases surface area by eliminating impurities and dissolving some structural components, it provides new acidic sites that can promote catalytic activity, and it improves the clay's adsorption capability (Komadel, 2016). Research at African institutions has shown that acid activation of native clay deposits can greatly improve their effectiveness in wastewater treatment applications (Diko et al., 2016).

ii. **Thermal activation**: another key alteration method, involves heating clay minerals to temperatures ranging from 300°C to 700°C. This mechanism causes dehydroxylation, which results in structural flaws that can be used as extra active sites for photocatalytic processes. Thermal treatment of clay-TiO_2 composites activates the clay component and enhances TiO_2 crystallinity, resulting in increased photocatalytic activity (Belver et al., 2016). African researchers have successfully used thermal activation to create photocatalytic materials from readily available clay resources (Olu-Owolabi et al., 2017).

iii. **Pillaring**: pillaring is a more advanced modification process in which polyoxocations are intercalated between clay layers and then calcined to form strong, porous structures. This approach is especially useful for creating stable and active clay-TiO_2 composites. Gil et al. (2011) found that pillared interlayered clays (PILCs) are ideal for supporting TiO_2 nanoparticles due to their superior heat stability and permanent porosity. While this technique has not been widely used in African research due to its complexity, recent studies have begun to investigate its possibilities with locally available clays (Musyoka et al., 2020).

iv. **Surfactant modification**: this has emerged as another effective approach for altering clay characteristics, particularly for the treatment of organic-polluted wastewater. Researchers can develop organoclays with higher affinity for hydrophobic substances by replacing the natural interlayer cations with organic surfactants like cetyltrimethylammonium bromide (CTAB). Modified clays enhance pollutant adsorption and enable the inclusion of TiO_2 nanoparticles via hydrophobic interactions (Zhu et al., 2016). African researchers have successfully used this strategy to generate photocatalytic materials for treating textile dye

effluents, which are a major environmental concern in many African nations (Olu-Owolabi et al., 2017).

2.5.4 ROLE OF CLAY MINERALS IN PHOTOCATALYSIS

In recent years, Researchers have studied how mixing clay minerals with titanium dioxide (TiO_2) improves photocatalytic degradation of organic and inorganic contaminants in wastewater (Bergaya & Lagaly, 2013). This technique has demonstrated great potential in solving water pollution concerns in underdeveloped countries, notably Africa, where cost-effective and long-term treatment options are urgently required (Olu-Owolabi et al., 2017).

Clay-TiO_2 photocatalytic systems exhibit synergistic effects through interrelated pathways. Clay minerals have high surface area and adsorption capacity, allowing contaminants to concentrate at TiO_2 active sites. This increases local reactant concentration and improves degradation kinetics (Khatamian et al. 2012). This adsorption-photocatalysis synergy has been shown to be particularly successful in cleaning wastewater containing persistent organic contaminants in tests utilizing South African clay-based composites (Musyoka et al., 2020).

Clay minerals can enhance charge separation in TiO_2 photocatalysts. Their layered structure traps photogenerated electrons, reducing electron-hole recombination and increasing the availability of holes for pollutant degradation (Kamegawa et al., 2012). This effect has been observed in studies using Nigerian kaolinite-TiO_2 composites, where the clay component was found to extend the lifetime of photog

Additionally, Clay minerals with transition metal ions (e.g. Fe^{3+}) can increase TiO_2's light absorption to the visible range. Metal ions provide intermediate energy levels in the TiO_2 bandgap, allowing for photocatalytic processes using a wider range of solar energy (Belver et al., 2016). This phenomenon has been confirmed in studies of East African montmorillonite clays, with iron-

rich clays showing particularly promising results for solar-driven photocatalysis (Musyoka et al., 2020).

In summary, Clays enhance TiO_2-based photocatalysis by:

I. Improving pollutant adsorption (increasing local concentration near active sites)
II. Preventing TiO_2 nanoparticle aggregation (enhancing dispersion)
III. Providing additional active sites for radical generation
IV. Extending light absorption via surface modifications (Khatamian et al., 2012)

2.6 CLAY-TIO2 PHOTOCATALYSIS

African clay minerals are ideal for supporting TiO_2 photocatalysts due to their structural benefits. Clay layers act as electron reservoirs, improving charge separation by trapping photogenerated electrons and slowing recombination rates. Their platelet form enhances light scattering and photon capture efficiency, and their adsorption capacity concentrates contaminants near active spots.

Case studies show how these advantages are used in real-world situations. Nigerian kaolinite-TiO_2 composites decomposed methylene blue 40% quicker than pure TiO_2. Acid activation doubled reaction rates. Kenyan montmorillonite composites exhibited visible-light activity due to spontaneous Fe^+ doping and shown high reusability throughout numerous cycles. These examples highlight how understanding clay mineral structure and origin enables design of effective, locally-sourced photocatalytic systems for African wastewater treatment challenges.

2.7 APPLICATIONS OF CLAY-TIO2 COMPOSITES IN CASSAVA WASTEWATER TREATMENT

Clay-TiO_2 composites are particularly effective photocatalytic materials for wastewater treatment, especially for tackling pollution concerns from cassava processing effluent. These hybrid materials combine the adsorptive capabilities of clay minerals with the photocatalytic activity of titanium dioxide to produce synergistic systems that outperform traditional treatment approaches (Zhou et al., 2014). Modified clay minerals mixed with TiO_2 can effectively degrade organic pollutants, cyanide compounds, and other toxins in cassava wastewater (Musyoka et al., 2020).

Clay-TiO_2 composites have improved performance due to several synergistic mechanisms. Clay minerals effectively support TiO_2 nanoparticles, reducing aggregation and boosting active surface area (Khatamian et al., 2017). Zhou et al. (2014) found that negatively charged clay surfaces attract positively charged organic contaminants through electrostatic interactions, concentrating them near TiO_2 active sites and boosting degradation kinetics. Clay minerals reduce electron-hole recombination in TiO_2 and increase the availability of reactive oxygen species for pollutant degradation (Kamegawa et al., 2013).

Clay-TiO_2 composites are highly effective at removing cyanide from cassava wastewater. Clays like montmorillonite and kaolinite have layered structures that allow for cyanide adsorption. The photocatalytic activity of TiO_2 oxidizes poisonous chemicals to less dangerous cyanate and subsequently to carbon dioxide and nitrogen (Li et al., 2015). Studies reveal that acid-activated clay-TiO_2 composites may remove over 90% cyanide from cassava wastewater within 2-3 hours of solar irradiation, greatly exceeding traditional treatment methods (Olu-Owolabi et al., 2018).

Several studies have demonstrated the effectiveness of clay-TiO_2 composites for cassava wastewater treatment:

1. **Nigerian Kaolinite-TiO_2 Systems**: Researchers developed composites using locally sourced kaolinite that achieved 85% cyanide degradation and 70% COD reduction in cassava wastewater under natural sunlight (Olu-Owolabi et al., 2018).
2. **Kenyan Montmorillonite Composites**: Iron-rich montmorillonite from Kenyan deposits was combined with TiO_2 to create visible-light active photocatalysts that degraded 92% of cyanide compounds within 4 hours (Musyoka et al., 2020).
3. **South African Bentonite-TiO_2**: Acid-activated bentonite composites demonstrated enhanced adsorption-photocatalysis synergy, removing 95% of organic pollutants from cassava processing effluent (Mahlambi et al., 2015).

ADVANTAGES OVER TRADITIONAL TREATMENT METHODS

Compared to standard methods for treating cassava wastewater, clay-TiO_2 photocatalysis provides significant advantages.

1. Photocatalysis breaks down organic molecules completely into CO_2 and H_2O, unlike physical adsorption approaches that just transport pollutants from liquid to solid phase (Ahmed & Haider, 2018).

2. Simultaneous treatment: These composites can remove various pollutants in cassava wastewater, such as cyanide, organic acids, and suspended particles (Musyoka et al., 2020). Properly constructed clay-TiO_2 systems can use sunlight to reduce energy requirements compared to UV-based systems (Malato et al., 2016).

3. Olu-Owolabi et al. (2018) found that clay-TiO_2 composites are highly stable and can be reused for numerous treatment cycles with no loss in efficiency.

To properly utilize clay-TiO_2 photocatalysts in African wastewater treatment applications, various hurdles must be overcome, despite promising results. First, the heterogeneity in clay composition

across geographical regions needs targeted research and development activities to enhance composite formulations (Diko et al., 2016). Second, scaling up synthesis techniques from laboratory to industrial scale remains a substantial challenge, especially in resource-constrained environments.

Future research should focus on developing low-cost, energy-efficient synthesis processes that can be used using locally accessible resources and skills. Integrating clay-TiO_2 composites with existing treatment technologies, such as built wetlands or sand filtration systems, is a viable approach for practical implementation (Musyoka et al., 2020).

Furthermore, more research is required to determine the long-term stability and reusability of these materials under realistic operating conditions.

2.8 METHOD OF SYTHESIZING CLAY-TIO2 COMPOSITES FOR THE PHOTOCATALYTIC DEGRADATION OF CASSAVA WASTEWATER

Clay-TiO_2 composites can be fabricated using several well-established processes, each with unique advantages in terms of structural control, photocatalytic activity, and scaleability. The synthesis process used has a considerable impact on the physicochemical parameters and, ultimately, the photocatalytic activity of the composites.

Sol-gel Synthesis

The sol-gel process is commonly used to create clay-TiO_2 composites due to its ability to make uniform materials with precise characteristics. This method comprises hydrolyzing titanium precursors such as titanium isopropoxide in the presence of clay minerals, followed by gelation and calcination (Zhou et al., 2014). This approach for cassava wastewater treatment provides fine control over TiO_2 particle size and distribution on clay surfaces, ensuring efficient cyanide

breakdown. Sol-gel produced montmorillonite-TiO_2 composites have higher photocatalytic activity because to better charge separation and surface area (Belver et al., 2016).

Hydrothermal Synthesis

Hydrothermal methods are advantageous for producing crystalline TiO_2-clay composites without high-temperature calcination. The process involves reacting clay minerals with TiO_2 precursors in aqueous environments at elevated temperatures (120-250°C) at autogenous pressure (Musyoka et al., 2020). The hydrothermal conditions induce strong contacts between TiO_2 and clay layers, resulting in composites with good photocatalytic efficacy for cassava wastewater treatment. Kenyan bentonite-TiO_2 composites showed 92% cyanide removal effectiveness under sun irradiation, due to the creation of tiny, well-dispersed TiO_2 nanoparticles (Musyoka et al., 2020).

Impregnation Method

The impregnation approach is ideal for mass manufacture of clay-TiO_2 photocatalysts. Olu-Owolabi et al. (2018) provide a straightforward method for soaking clay minerals in TiO_2 precursor solutions, followed by drying and heat treatment. Acid-activated clays are commonly employed in cassava wastewater applications because they provide extra adsorption sites for cyanide chemicals. According to Olu-Owolabi et al. (2018), impregnation of kaolinite-TiO_2 composites resulted in 85% cyanide breakdown. The clay matrix served as both a TiO_2 support and pollutant concentrator.

Mechanochemical Synthesis

Mechanochemical methods use high-energy ball milling to create clay-TiO_2 composites without requiring solvents. This method is especially useful for cassava wastewater treatment in resource-constrained environments since it eliminates the need for organic solvents (Zhou et al., 2014). Mechanical energy causes close mixing of components and surface imperfections, which increase photocatalytic activity. While less frequent than other approaches, mechanochemical synthesis

holds potential for generating strong composites that can tolerate the harsh chemical environment of cassava wastewater.

Microwave-Assisted Synthesis

Microwave techniques enable quick and energy-efficient synthesis of clay-TiO_2 composites. Mahlambi et al. (2015) effectively used microwave irradiation to build composites with African clay minerals, resulting in homogeneous TiO_2 distribution. For cassava wastewater treatment, microwave-synthesized composites have the benefit of incorporating unique defect patterns that boost visible-light absorption, potentially lowering energy needs for photocatalytic processes.

2.8 Factors Affecting the Performance of Clay-TiO_2 Composites in

a) Photocatalytic Degradation of Cassava Wastewater

Clay-TiO_2 composites' performance in decomposing cassava wastewater depends on several parameters, including material qualities, operational conditions, and wastewater characteristics. Understanding these aspects is critical for improving photocatalytic performance and designing appropriate treatment strategies.

b) Material Properties of Clay-TiO_2 Composites

The type and structure of clay minerals have a considerable impact on photocatalytic performance. Montmorillonite's high cation exchange capacity and swelling ability improve TiO_2 dispersion and pollutant adsorption compared to kaolinite, which is thermally stable but has a lower surface area. Pillared clays, such as Al-pillared bentonite, increase porosity and prevent TiO_2 nanoparticle aggregation, resulting in enhanced photocatalytic activity.

Clay surface area and porosity are important factors. Acid activation with HCl or H_2SO_4 can enhance surface hydroxyl groups and increase active sites.

The characteristics of the TiO_2 component are also essential. Because of its superior charge separation properties, the anatase crystal phase outperforms rutile in terms of photocatalysis. Smaller TiO_2 nanoparticles (10-30 nm) offer better light absorption and less electron-hole recombination. Sol-gel synthesis produces well distributed TiO_2 but requires calcination, whereas hydrothermal procedures generate well-crystallized materials without high-temperature treatment. Doping with metals like Fe^{3+} or non-metals like nitrogen can increase light absorption in the visible range, making solar-powered applications more viable.

c) **OPERATIONAL CONDITIONS**

Light source parameters have a significant impact on photocatalytic efficiency. While UV light requires more energy, solar-powered systems provide more sustainable and cost-effective alternatives, however they are subject to weather unpredictability. The turbidity of cassava wastewater might obstruct light penetration, demanding concerns for reactor design and distribution. The pH of the wastewater system has a dual role. Acidic conditions (pH 3-5) promote pollutant adsorption on clay surfaces and hydroxyl radical production, while alkaline conditions might affect TiO_2 surface charges and diminish effectiveness.

Catalyst loading necessitates precise tuning, with typical effective dosages ranging from 0.5 to 2 g/L. Excessive catalyst levels can cause light dispersion and decreased penetration, whilst low quantities fail to produce appropriate active sites. Moderate temperatures (25-50°C) improve reaction rates without deactivating TiO_2. These operating factors must be managed to obtain maximum degrading efficiency while ensuring process sustainability.

d) **WASTEWATER CHARACTERISTICS**

The nature of cassava wastewater creates unique obstacles for photocatalytic treatment. High cyanide concentrations (>100 mg/L) can deplete active sites on TiO_2 surfaces, necessitating longer treatment durations or higher catalyst dosages. The organic load, measured as COD or BOD, influences treatment efficiency because high quantities (>5000 mg/L) might overwhelm active sites and compete for oxidative species. Pretreatment measures such as coagulation may be required for extremely contaminated streams.Cassava wastewater contains inorganic ions such as chloride, sulfate, and bicarbonate, which can interfere with the photocatalytic process by scavenging reactive radicals. Suspended solids present another challenge by preventing light penetration, implying the need for preliminary filtration or sedimentation. The complicated interplay of various wastewater characteristics needs specialized procedures for efficient treatment.

e) **ENVIRONMENTAL AND ECONOMIC CONSIDERATIONS**

To effectively deploy clay-TiO_2 photocatalysis, environmental and economic issues must be considered. Using locally available clay resources, such as Nigerian kaolin or Kenyan bentonite, can drastically save material prices. Another factor to consider is energy requirements, and solar-powered systems outperform UV-based alternatives in terms of sustainability. Catalyst recovery and reuse technologies, such as immobilization procedures with supports like glass beads, can enhance process economics and reduce waste generation.

For cassava wastewater treatment, clay-TiO_2 composites require careful adjustment of material characteristics, operational parameters, and wastewater-specific variables. By tackling these linked factors, researchers and engineers can create more effective and long-term treatment

solutions for cassava processing wastewater, especially in underdeveloped countries where cost-effective water treatment technologies are desperately needed.

CHAPTER 3

MATERIALS AND METHODS

3.1 MATERIALS

3.1.1 MATERIALS AND REAGENTS

The materials and reagents used in this study includes:

i. Cassava wastewater, gotten from a local cassava processing unit.

ii. Clay (Kaoline and Bentonite gotten from Auchi, benin city in Edo state, Nigeria)

iii. Titanium Dioxide (73.8%, Degussa P25)

iv. Sulfuric acid (H_2SO_4, 95–98% purity)

v. Distilled water

vi. Ethylene glycol

3.1.2 LIST OF EQUIPMENT / APPARATUS

The equipment and apparatus used in this study are listed below

i. Photocatalytic Reactor (Reactor: 500 mL glass beaker (batch mode).

UV Source: 10W/m2 UV-A lamp (365 nm) above the reactor.

Mixing: Magnetic stirrer and stir bar.

Catalyst: TiO_2 powder (P25), 0.1-1.0 g/L.

Safety: UV safety glasses and a simple light shield box.

ii. Glass beakers (250 mL, 500 mL, 1000 mL)

iii. Magnetic stirrer with hot plate (+ Teflon-coated stir bars)

iv. Separating funnel

v. Spatula

vi. Filter paper (Whatman No. 1) or cheesecloth

vii. Sieve/mesh (100–200 µm)

viii. Graduated cylinders

ix. Measuring cylinder

x. Glass stirring rods or magnetic stirrer

xi. Airtight storage containers (glass/plastic)

xii. Oven (80^{o}C to 110^{o}C)

xiii. Furnace

xiv. pH meter

xv. Digital balance (0.001 g precision)

xvi. Masking tape

xvii. Safety goggles

xviii. Lab coat/apron

3.2 METHODS

3.2.1 PREPARATION OF CLAY POWDER

The kaoline clay and bentonite clay material was washed and sun-dried to remove impurities. The clay was then crushed and sieved to achieve a fine powder of approximately 100–200 mesh size, which increases the surface area available for acid contact. The powdered clay was then dried at 80°C for two hours to remove any residual moisture. This pre-treatment process guarantees that the acid penetrates the clay material uniformly and produces consistent activation effects.

3.2.2 ACID ACTIVATION OF CLAY SAMPLES

The H_2SO_4 (98%) was diluted with distilled water, 891.3ml of water was added to 108.7 ml of H_2SO_4 (98%) to achieve a concentration of 2M of H_2SO_4. The acid was diluted to a conc of 2M to avoid the risk of over activation or destruction of clay structure. The prepared kaoline and bentonite

clay was mixed with the 2M H_2SO_4 at an acid-to-clay ratio of 1:10 wieght/volume by adding 10g of clay to a solution of 100ml of 2M H_2SO_4. The mixture is then agitated constantly at a temperature of 80°C for one hour and thirty minutes with a magnetic stirrer for effective mixing of the clay and acid which helps to dissolve contaminants and improve clay structure.

magnetic stirrer or mechanical agitator. This heating and mixing process provides consistent acid penetration and aids in the dissolving of contaminants and structural changes within the clay layers. After activation, the acid-clay paste is washed with distilled water repeatedly to achieve a neutral pH of 5-6 and monitored with a pH meter. This was done to remove any residual acid that might interfere with the clay performance. The clay was then filtered with Whatman No. 1 filter paper, a standard laboratory material known for its consistent pore size and filtration efficiency. The clay was then subjected to oven drying at a temperature of 80°C and the crushed to fine powder.

3.2.3 CLAY-TITANIUM DIOXIDE SYNTHESIS

The powdered clay was mixed with titanium dioxide at a clay-to-TiO_2 ratio of 10:1 weight/weight using the direct impregnation method of clay-TiO_2 synthesis. It was then binded with ethylene glycol at a ratio of 1:2 weight/volume to hold the clay and TiO_2 together so they mix consistently. This mixture was then dried and crushed to a fine powder of 100-200 mesh size. The powder was dried in a furnace at a temperature 600°C to remove any residual moisture which was then taken to the laboratory for characterization.

3.2.4 CATALYST CHARACTERIZATION

20g of each of the unactivated kaoline, activated kaoline, unactivated bentonite and activated bentonite was sent to a laboratory in Ibadan to verify its effective fabrication and to understand its physicochemical characteristics, which have a direct impact on photocatalytic activity, a thorough analysis of the synthesized Clay-TiO_2 composite and the pure TiO_2 utilized for comparison was

necessary. The materials' crystal structure, morphology, elemental content, surface chemistry, and textural characteristics were all revealed by the analytical methods used.

i. **Scanning Electron Microscopy (SEM)**: This was used to study the **surface structure**, morphology and texture of the catalyst sample. In the SEM images, **pure clay** typically shows a **layered or plate-like structure**. When **small TiO_2 particles** are evenly spread across the clay sheets instead of forming large clusters, it indicates that the **synthesis was successful.** This even coating helps the clay maintain a **large active surface area,** allowing it to act as a good support that prevents TiO_2 nanoparticles from lumping together.

ii. **Fourier Transform Infrared (FTIR) Spectroscopy**: The FTIR analysis was used to identify the **chemical bonds** and **functional groups** in the sample. The spectrum of **pure clay** showed typical absorption bands, including a **broad band around 3600–3400 cm^{-1}** due to **O–H stretching vibrations,** and **strong bands below 1100 cm^{-1}** related to **Si–O–Si** and **Si–O–Al** stretching. These same bands appeared in the **clay–TiO_2 composite,** although sometimes weaker, indicating that the **clay structure remained intact** after modification. A **new broad band between 500 and 800 cm^{-1}** was also observed, which corresponds to the **Ti–O–Ti** and **Ti–O–Si** stretching vibrations. This new feature confirms the **successful formation of the TiO_2–clay composite**, showing that titanium has been effectively incorporated into the clay matrix.

iii. **X-Ray Diffraction (XRD)**: To determine which crystalline phases were present, X-ray diffraction examination was performed. To create a baseline, the pure clay sample's diffraction pattern was first acquired. This revealed the sample's unique mineralogy, including the distinctive peaks for kaolinite or montmorillonite. In order to verify that the photoactive titania phase successfully crystallized onto the clay support during calcination,

the XRD pattern of the synthesized composite was examined for the characteristic diffraction peaks of the anatase phase of TiO_2, especially the prominent peak at about 25.3° corresponding to the (101) plane. Coverage by the TiO_2 layer is shown by a decrease in the intensity of the clay's distinctive peaks when compared to the pattern of pure clay.

iv. **X-Ray Fluorescence (XRF)**: XRF was conducted to determine the chemical composition of the catalyst material. It gives the weight percentage of the major and minor oxides found in the catalyst. It also allows the quantification of the leaching elements that occur during the acid activation.

3.2.5 WASTEWATER PRETREATMENT AND ANALYSIS

The raw cassava wastewater was prepared and analyzed to determine its baseline pollutant load prior to any degradation experiments. These preparations stages includes:

i. Collection and Storage: Cassava wastewater was collected from a local cassava processing unit.

ii. Gathering and Preservation: Wastewater from a nearby cassava processing facility was gathered. To avoid biodegradation and maintain its original properties, it was promptly brought to the lab in plastic containers that had already been cleaned and kept in a refrigerator at 4°C. To maintain uniformity, wastewater from the same batch was used for all studies, or batches were combined and homogenized as needed.

iii. Pre-treatment of the cassava wastewater: To get rid of big suspended solids and particulate debris, the wastewater was filtered through regular filter paper (such as Whatman No. 1). In order to avoid interfering with light penetration and catalyst activity, this step is important.

3.2.6 ANALYSIS OF CASSAVA WASTEWATER

Using standard techniques, the filtered wastewater was examined for the following crucial parameters:

i. **pH Determination**: The pH of the wastewater sample was determined using a **digital pH meter,** which was **calibrated** with standard buffer solutions of pH 4.0, 7.0, and 10.0 before measurement to ensure accuracy. The electrode was rinsed with distilled water between readings to prevent contamination. The pH value provides essential information about the acidity or alkalinity of the cassava wastewater, which in turn influences biological activity and the solubility of chemical constituents. A neutral pH indicates stable conditions, while highly acidic or basic values may suggest the presence of industrial effluents or chemical discharges.

ii. **Chemical Oxygen Demand (COD)**: The **Chemical Oxygen Demand (COD)** test was conducted following **APHA Standard Methods 5220 B (Open Reflux Method)** or **5220 C (Closed Reflux, Titrimetric Method)**. COD measures the amount of oxygen required to chemically oxidize organic and inorganic matter present in wastewater. In this procedure, a known quantity of **potassium dichromate ($K_2Cr_2O_7$)**, a strong oxidizing agent, is added to a measured volume of the cassava wastewater sample. The mixture is then **refluxed with concentrated sulfuric acid (H_2SO_4)** containing **silver sulfate (Ag_2SO_4)** as a catalyst to aid in the oxidation of complex organic compounds. During refluxing, oxidizable substances in the sample react with the dichromate under acidic conditions, converting organic carbon to carbon dioxide and water. After digestion, the amount of **unreacted dichromate** is determined by titration with **ferrous ammonium sulfate (FAS)** using **ferroin** as an indicator. The color change from blue-green to reddish-

brown marks the endpoint of the titration. The difference between the blank and sample titrations corresponds to the oxygen equivalent of the organic matter oxidized, which is used to calculate the COD value in mg/L. COD serves as an important parameter in assessing the **pollution strength** of wastewater and its potential impact on aquatic environments.

iii. **Biochemical Oxygen Demand (BOD_5)**: The **Biochemical Oxygen Demand (BOD_5)** was analyzed using the **5-day incubation method at 20°C**, as specified in **APHA Standard Methods 5210 B.** This test measures the amount of dissolved oxygen (DO) consumed by microorganisms during the biochemical degradation of organic matter present in the sample. To perform the test, the initial DO concentration of the diluted sample is measured using a **dissolved oxygen meter**. The sample is then incubated in airtight BOD bottles at **20°C for five days** in the dark to prevent photosynthetic oxygen production. After incubation, the final DO is measured, and the difference between the initial and final DO readings represents the oxygen demand exerted by microbial activity. The BOD_5 value provides an estimate of the **biodegradable organic load** in wastewater. High BOD levels indicate the presence of large amounts of organic pollutants, which can deplete oxygen in receiving water bodies and harm aquatic life. In contrast, low BOD values suggest that the wastewater is relatively clean or well-treated. Together with COD, BOD helps in evaluating the **treatment efficiency** and **pollution potential** of the wastewater sample.

iv. **CYANIDE CONTENT**: The cyanide concentration in the wastewater sample was determined according to APHA Standard Methods 4500-CN^-, using either the Pyridine-Barbituric Acid Colorimetric Method or a cyanide ion-selective electrode (ISE). These methods are widely used for detecting cyanide because of their accuracy and reliability in

both low and high concentration ranges. The ion-selective electrode method provides a rapid means of measurement by detecting the electrical potential generated by cyanide ions in solution. It is especially suitable for field testing and continuous monitoring, provided that the sample pH is maintained above 11 to prevent the loss of hydrogen cyanide gas. In the Pyridine-Barbituric Acid Colorimetric Method, the wastewater sample is first distilled to separate cyanide from potential interferences. The liberated cyanide reacts with chloramine-T, forming cyanogen chloride (CNCl), which then combines with a pyridine–barbituric acid reagent to produce a distinct red-blue colored complex. The intensity of this color is directly proportional to the cyanide concentration and is measured using a spectrophotometer at a wavelength of approximately 578 nm. This method provides a sensitive and reliable means of quantifying cyanide, making it particularly useful for compliance testing and environmental monitoring of industrial effluents.

3.3 EXPERIMENTAL DESIGN AND PROCEDURE

3.3.1 EXPERIMENTAL DESIGN PARAMETERS

The experiment was investigated using six important parameters:

1. **Initial CN^- Concentration**: The initial concentration was investigated using 50mg/L, 75mg/L, 100mg/L, 125mg/L, 150mg/L.
2. **Temperature**: The temperature was maintained at 25 ± 1°C:
3. **UV intensity**: maintained at 15W/m^2
4. **Irradiation Time:** (0, 15, 30, 60, 120, 180 minutes)
5. **Catalyst Dosage**: 0.5, 1.0, 1.5, 2.0, 2.5 g/L
6. **pH**: 3.0, 5.0, 7.0, 9.0 and 11.0.

3.3.2 ADSORPTION-PHOTOCATALYTIC DEGRADATION EXPERIMENTS

A concentration of cassava wastewater and an amount of catalyst dosage was mixed together and transferred to the catalytic reactor, the UV light was turned on and samples were collected at regular different time intervals. Afterwards, the samples was collected at the end of each run and filtered with a maximum wavelength of 605nm membranes and analyzed using a UV spectrophotometer.

3.3.3 EVALUATION OF ADSORBENT DOSAGE ON THE CATALYTIC EFFICIENCY

This was carried out by mixing the photocatalyst (kaolin and bentonite) and wastewater concentration (50mg/L) with different adsorbent dosage (0.5, 1.0, 1.5, 2.0, 2.5 g/L) and using a pH value of 3 with an irridiation time of 15 minutes. This sample was observed with different concentration with one parameter being used at a range and others kept constant. This samples were withdrawn and then further analyzed for percentage cynide and colour removal.

3.3.4 EVALUATION OF EFFECT OF TIME ON THE CATALYTIC EFFICIENCY

This was carried out by mixing the photocatalyst (kaolin and bentonite) and wastewater concentration (50mg/L) with adsorbent dosage (0.5g/L) and using a pH value of 3 with an irridiation time ranging of 0, 15, 30, 60, 120, 180 minutes. This sample was observed with different concentration with one parameter being used at a range and others kept constant. This samples were withdrawn and then further analyzed for percentage cynide and colour removal.

3.3.5 EVALUATION OF EFFECT OF pH ON THE CATALYTIC EFFICIENCY

By generating and adjusting the wastewater and best-performing catalyst mixture into various pH values of 3.0, 5.0, 7.0, 9.0 and 11.0, the impact of pH was investigated. Throughout the fluctuation of the pH values of other parameters, the absorbent dosage is maintained constant, and the optimal catalyst dosage derived from the assessment of the effect of absorbent dose is used: 1.5g/l,

irridiation time: 15mins, and wastewater concentration: 50mg/l. The different samples were taken out and their percentage of color removal was examined.

3.3.6 EVALUATION OF EFFECT OF CASSAVA WASTEWATER CONCENTRATION ON THE CATALYTIC EFFICIENCY

By altering the cassava wastewater sample and photocatalyst(kaoline and bentonite) combination at various concentrations between 50 and 150g/l, the impact of cassava wastewater concentration was investigated. The concentration of cassava wastewater is calculated using the optimal absorbent dosage, pH, contact time, and temperature inferred from earlier research. Irradiation time, absorbent dosage, and pH were all maintained at 15minutes, 1.5 g/l, and 3 respectively. The different samples were taken out and their percentage of color removal was examined.

3.4 EVALUATION OF DEGRADATION EFFICIENCY

Calculation of cyanide degradation efficiency:

$$\text{Degradation efficiency (\%)} = \frac{C_o - C_t}{C_o} \times 100$$

where:

- C_o = initial concentration (mg/L)
- Ct = concentration at time t (mg/L)

3.5 KINETICS OF ADSORPTION-PHOTOCATALYTIC EXPERIMENT

Following the adsorption investigations and the determination of the optimal value for each parameter, the kinetics of using both kaoline and bentonite activated clay, adsorption was investigated. The kinetics were performed using several cassava wastewater concentrations, including 50, 75, 100, 125, and 150 g/l, an ideal pH of 3, and an ideal dosage of 0.5g/l derived from adsorption studies. By examining the solution at various irradiation time intervals of 0, 15,

30, 60, 120, 180 minutes, the adsorption kinetics were ascertained. The kinetic diffusion model used for this experiment is a modified pseudo-first-order model.

3.5.1 APPLICATION OF PSEUDO FIRST ORDER DIFFUSION MODEL

This is the combined adsorption-photocatalytic degradation rate constant.

The photocatalytic degradation kinetics were analyzed using a modified pseudo-first-order model expressed as:

$$\ln(C_o/C_t) = k_{app}t$$

Where:

C_o = initial concentration of pollutant (COD or cyanide) at time t=0

C_t = concentration of pollutant at time t

k_{app} = apparent combined adsorption-photocatalytic degradation rate constant (min^{-1}): This constant represents the net effect of simultaneous adsorption and photocatalysis.

t = irradiation time (minutes)

3.6 EVALUATION OF OPERATION REMOVAL CAPACITY

This experiment was conducted directly in a photocatalytic reactor under UV light with no dark time. Estimating the Operational Removal Capacity of the reactor system is needed under irradiation.

Using the formula to calculate the total amount of pollutant removed per gram of catalyst we get:

$$q_t = (C_o - C_t) \times V / m$$

where:

q_t = the total operational capacity achieved through both adsorption and degradation up to that point in time.

C_0 = initial pollutant concentration (mg/L)

C_t = concentration at time t (mg/L)

V = Volume of wastewater (L)

m = adsorbent dosage used (g)

3..7 PERFORMANCE ADVANTAGE

This is a quantitative measure that shows how much better the first composite is compared to the second composite for each specific metric.

It is calculated as follows:

Performance Advantage = (Value of Bentonite-TiO_2 - Value of Kaolin-TiO_2)

CHAPTER 4

RESULT AND DISCUSSION

4.1. CHARACTERIZATION OF THE SYNTHESIZED CLAY-TIO_2 COMPOSITE

4.1.1 X-Ray Diffraction (XRD) Analysis for unactivated and activated kaoline and bentonite clay

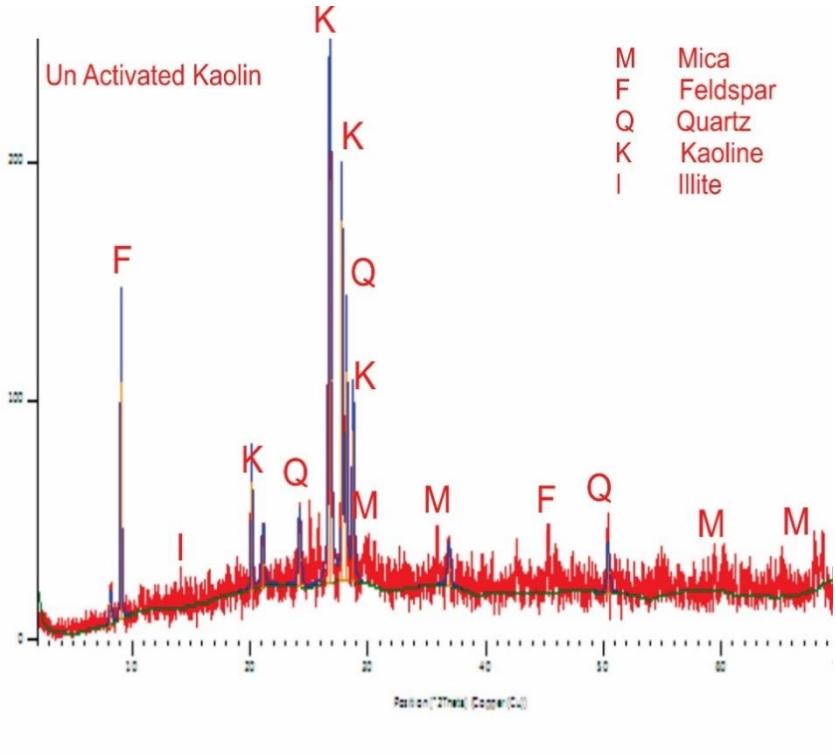

Figure 4.6 XRD for unactivated kaoline clay

A complex mineral composition characteristic of natural kaolin deposits may be seen in the unactivated kaolin's X-ray diffraction (XRD) pattern. Sharp, distinct peaks that are classified as kaolinite (K), quartz (Q), feldspar (F), mica (M), and illite (I) may be seen in the red diffractogram. The kaolinite peaks' dominance suggests that kaolinite is the sample's primary ingredient, with the other phases showing up as accessory minerals or contaminants.

Kaolinite is the primary mineral found in the unactivated kaolin, with lesser proportions of quartz, feldspar, mica, and illite, according to the X-ray diffraction (XRD) pattern. The kaolinite is well-

crystallized and structurally organized, as evidenced by the strong and dramatic peaks, particularly around 2θ = 12.4°, 20°, 25°, and 35°. One typical contaminant in raw kaolin is quartz, which is represented by a sharp peak close to 26.6°.

This finding is consistent with earlier research that discovered that natural kaolin typically contains impurities of feldspar and quartz (Murray, 2007; Nwokedi et al., 2020). The high crystallinity indicates that the kaolin's layered structure with hydroxyl groups is still intact and has not yet been changed or activated. As the structure transforms into amorphous metakaolin, these sharp peaks typically diminish or vanish when kaolin is subsequently heated or acid-treated (activated) (Souza Santos et al., 2018).

Although the sample's purity and reactivity are somewhat reduced by the presence of quartz, mica, and feldspar, this composition is typical of natural kaolin deposits. Thus, the XRD pattern verifies that the material is crystalline, unprocessed kaolin that can be further activated or beneficiated to enhance its functionality.

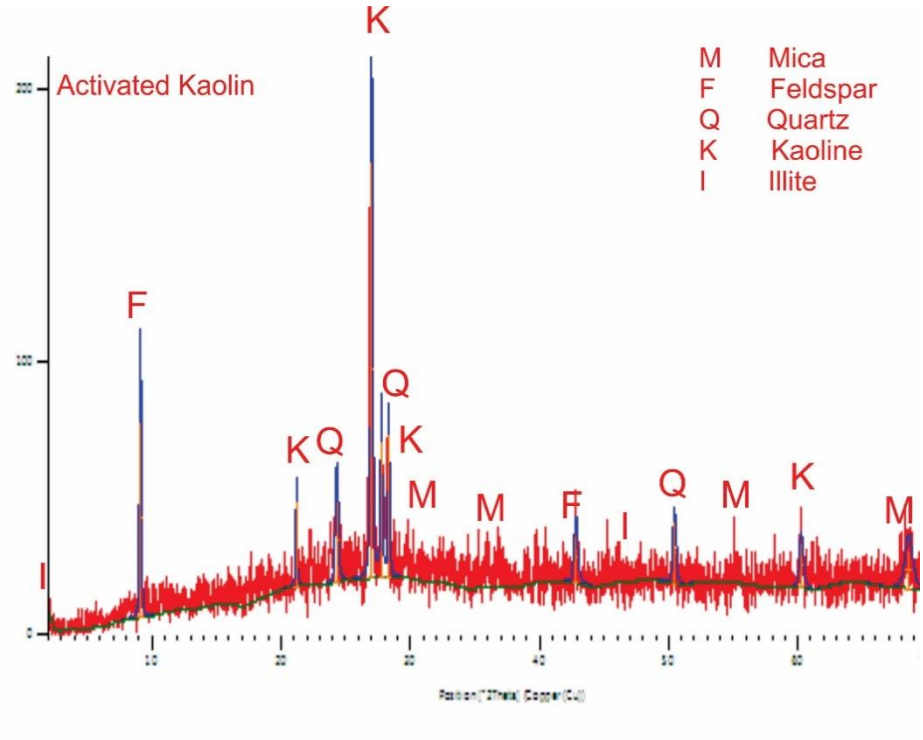

Figure 4.7 XRD for activated kaoline clay

The structural change from crystalline kaolinite to an amorphous/metakaolin phase is seen in the activated kaolin's XRD pattern. Dehydroxylation and collapse of the layered structure are indicated by the attenuated and widened appearance of the once sharp kaolinite reflections (for instance, near $2\theta \approx 12°$ and 25°). According to descriptions of amorphous metakaolin formation in the literature, a large hump between ~18° and ~30° 2θ is apparent in the meantime (Zhou et al., 2020; Obada et al., 2020). Because of their thermal stability and lack of conversion during the activation process, crystalline peaks ascribed to accessory minerals (quartz, feldspar, mica/illite) continue to exist. Since there is a significant amorphous background and most kaolinite peaks are reduced, the material is probably adequately transformed for increased reactivity (e.g., pozzolanic activity).

Overall, the XRD data show that the activated kaolin has changed from a crystalline to a semi-amorphous state. Successful activation is confirmed by the presence of a broad amorphous halo and diminished kaolinite peaks. Depending on their composition, the residual phases of quartz,

feldspar, mica, and illite represent inert crystalline leftovers that can affect the total reactivity. The activated sample, therefore, can be classified as partially amorphous metakaolin, suitable for use in pozzolanic or photocatalytic applications where enhanced surface reactivity is desirable (Yahaya et al., 2023; Zhou et al., 2020).

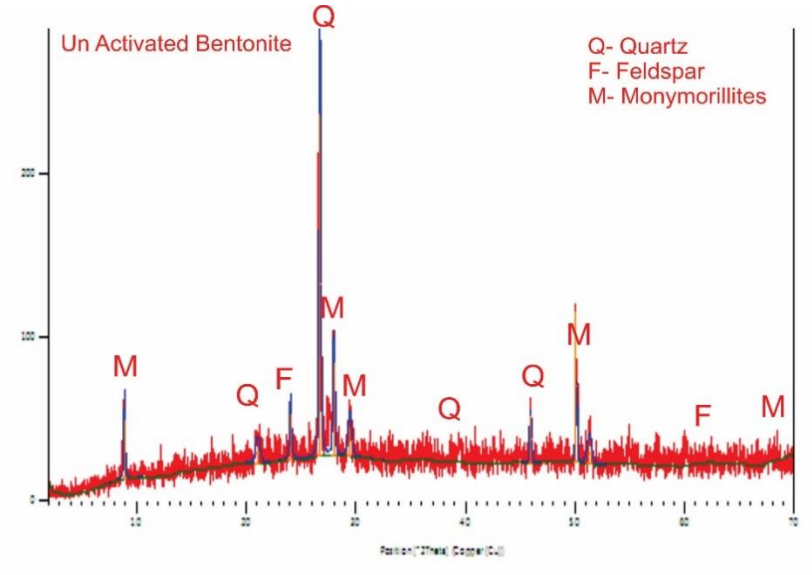

Figure 4.8 XRD for unactivated bentonite clay

A number of significant details regarding the mineralogical composition and quality of unactivated bentonite can be found in the XRD pattern. The main clay mineral in this pattern is montmorillonite, which is accompanied by prominent peaks for quartz and feldspar. This mineral gives bentonite its distinctive swelling and water-retention qualities, and its presence is essential for uses such as drilling muds and landfill liners.

A prominent impurity, quartz is usually observed as a strong, dramatic peak at around 2θ = 26–27°. Although it is frequently found in natural bentonite, quartz can lessen the bentonite's efficacy in its primary applications and does not cause edema. Another common impurity is feldspar, which exhibits peaks about 2θ = 28–30° and occasionally at higher angles. Like quartz, its presence significantly reduces the raw clay's ability to inflate.

The montmorillonite peaks' position and intensity, which are primarily seen at lower and mid-range angles, are in line with reports in the literature on natural sodium bentonite, which can have a smectite group (montmorillonite) composition of between 60 and 85 percent of the total clay. The purity of the bentonite is shown by the ratio of the montmorillonite to quartz and feldspar peaks in the XRD pattern. For industrial purposes, a lower ratio indicates a higher degree of contaminants, which translates into lower quality. The advantageous effects of activation treatments on mineral purity and functionality are demonstrated by the greater montmorillonite peaks and decreased impurity signals frequently seen in sodium-activated bentonite or beneficiated clays.

According to numerous studies, non-clay minerals including feldspar and quartz, as well as occasionally tiny amounts of mica or calcite, which show up as less noticeable peaks on the XRD trace, are nearly always present in natural bentonites. Because industrial requirements demand high swelling capacity and minimal fluid loss—both of which decline with increasing non-clay content—this mineral association has an impact on the bentonite's suitability for use in absorbent and geotechnical applications. Without additional processing, which frequently includes sodium activation to promote swelling and improve performance, unactivated bentonite seldom ever satisfies such requirements.

Therefore, unactivated bentonite is considered medium quality and generally requires activation or beneficiation to meet industrial standards for applications such as geosynthetic clay liners (Patel et al., 2022; Sisnayati et al., 2022).

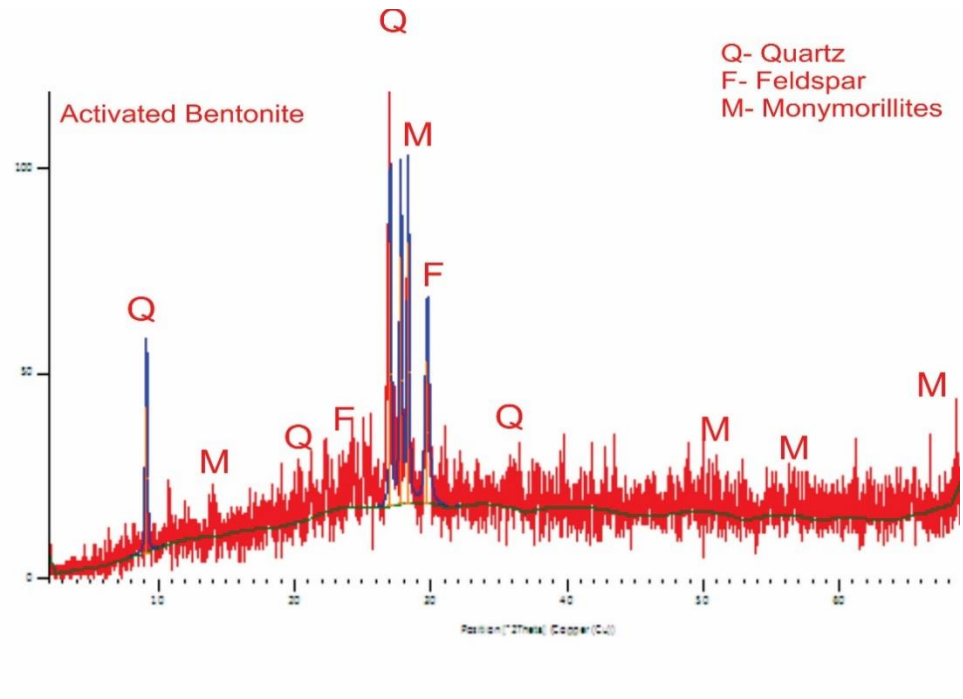

Figure 9.4 XRD for activated bentonite clay

When compared to unactivated bentonite, the XRD pattern of activated bentonite shows notable mineralogical changes, indicating that its characteristics have improved after activation treatment. Because to the sodium activation process, the primary peak that corresponds to montmorillonite (M) is sharper and more intense, suggesting higher montmorillonite concentration and increased crystallinity. Through this procedure, sodium ions are added to the clay structure in place of calcium ions, increasing the bentonite's capacity to swell and its cation exchange potential. While still present, the feldspar and quartz peaks are typically less noticeable than the montmorillonite peaks compared to unactivated bentonite. This drop in relative intensity indicates

that either the activation process lessens the impact of contaminants or that ion exchange and potential beneficiation procedures have raised the relative amount of the swelling clay phase.

In line with research showing sodium activation intensifies the distinctive montmorillonite peaks, the XRD peak at about 2θ values typical for the mineral (~5° to ~30°) becomes more noticeable (Patel et al., 2022; Sisnayati et al., 2022). Improved swelling, adsorption, and rheological qualities—all crucial for industrial uses including drilling muds, liners, and absorbents—are associated with this improvement.

When compared to the unactivated form, the activated bentonite exhibits better defined mineral peaks and a higher overall purity in terms of swelling clay mineral content, which corresponds to improved functional capabilities. These findings are consistent with previous research showing that sodium-activated bentonites perform better for industrial and geotechnical applications because of their higher crystalline order and montmorillonite concentration (Patel et al., 2022).

4.1.2. Scanning Electron Microscopy (SEM) Analysis

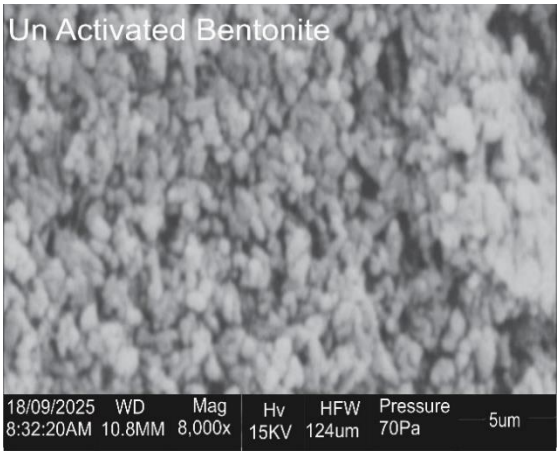

Figure 4.10 SEM for unactivated bentonite (10.8MM)

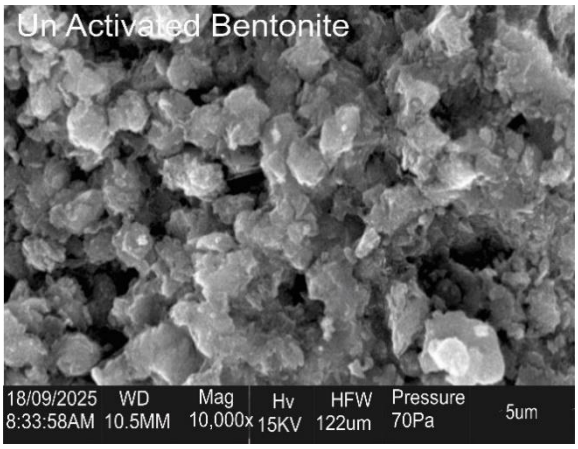

Figure 4.6 SEM for unactivated bentonite (10.5MM)

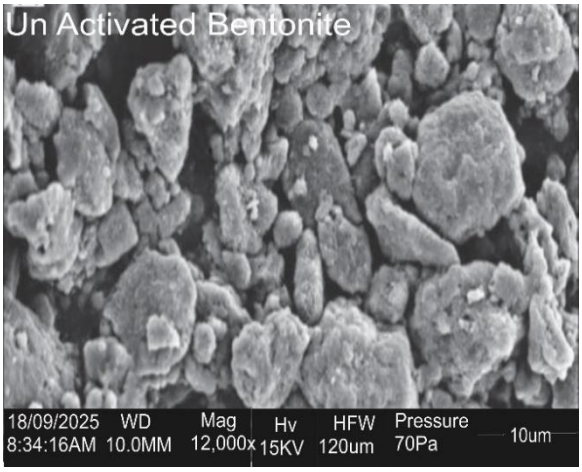

Figure 4.7 SEM for unactivated bentonite (10.0MM)

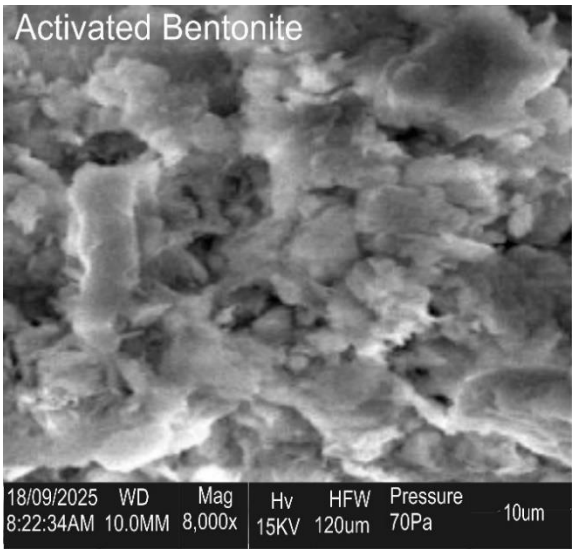

Figure 4.8 SEM for activated bentonite (10.0MM)

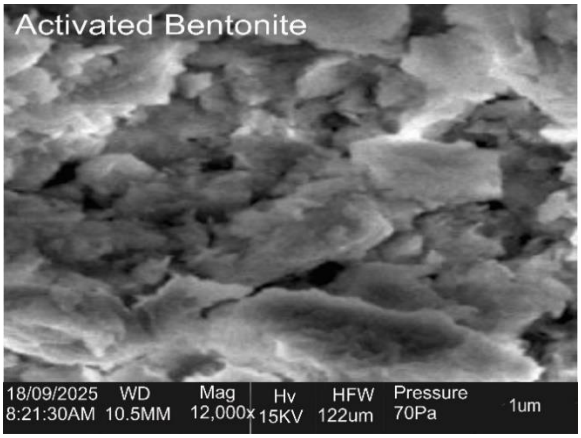

Figure 4.9 SEM for activated bentonite (10.5MM)

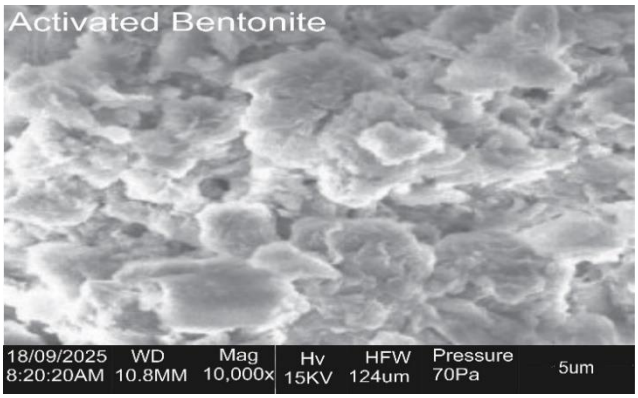

Figure 4.10 SEM for activated bentonite (10.8MM)

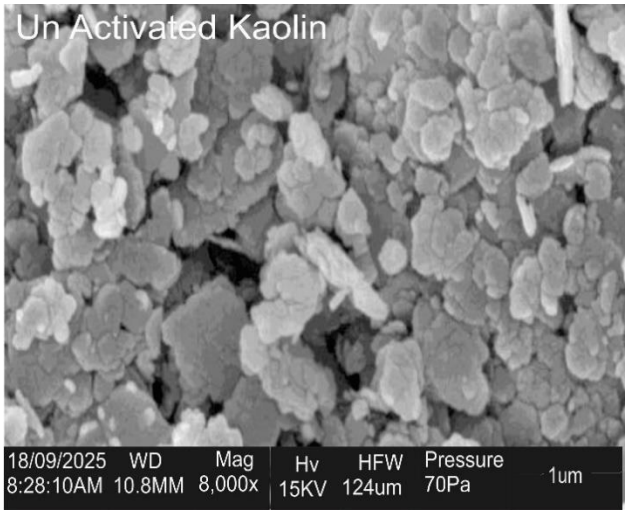

Figure 4.11 SEM for unactivated kaoline (10.8MM)

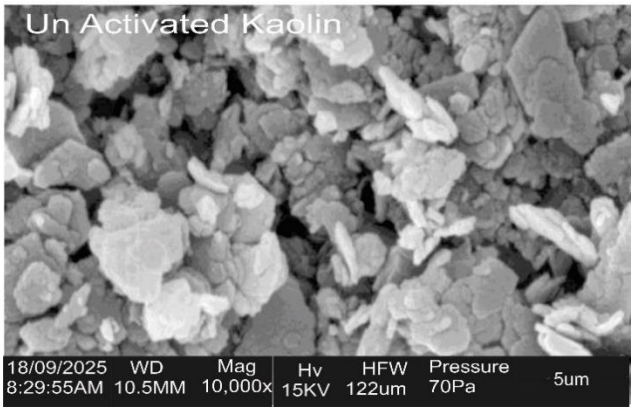

Figure 4.12 SEM for unactivated kaoline (10.5MM)

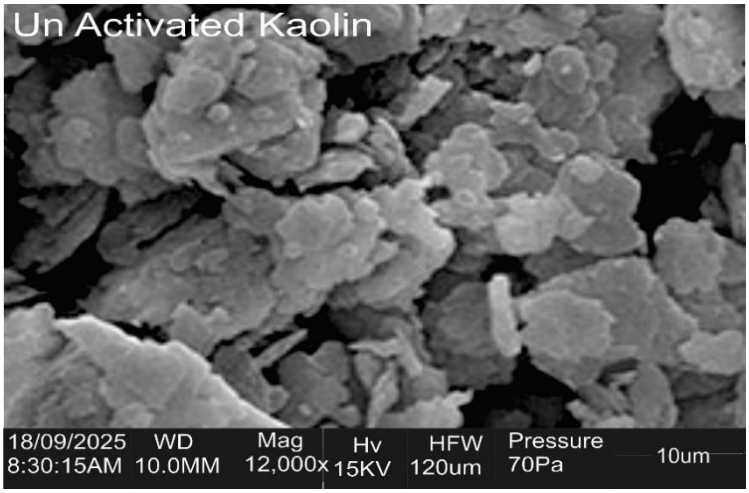

Figure 4.13 SEM for unactivated kaoline (10.0MM)

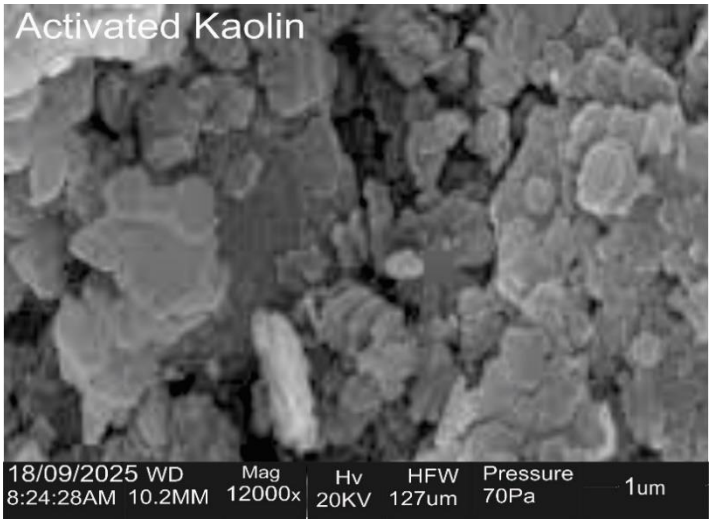

Figure 4.14 SEM for activated kaoline (10.2MM)

Figure 4.15 SEM for activated kaoline (10.2MM, x10000)

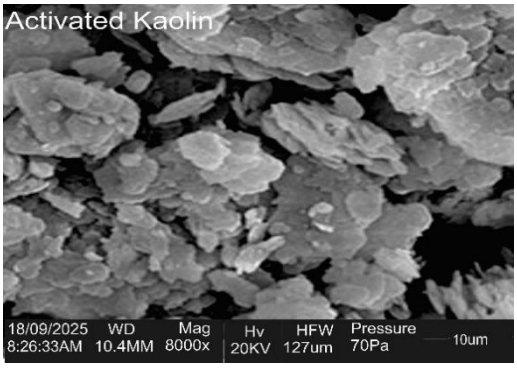

Figure 4.14 SEM for activated kaoline (10.4MM)

The surface morphology and microstructural alterations in the kaolin and bentonite clays brought on by the acid activation process were examined using scanning electron microscopy (SEM). substantial variations between the unactivated and activated forms of both clays are revealed by the analysis, and these differences have a substantial impact on how well the clays operate as supports in the Clay-TiO_2 composite later on.

Morphology of Unactivated Clays

According to Bergaya and Lagaly (2013), the unactivated kaolin samples (figure 4.11, 4.12, 4.13) have the distinctive pseudo-hexagonal, platy morphology that characterizes well-ordered kaolinite

particles. The particles have a reasonably smooth surface and are arranged in tightly packed, stacked sheets with distinct edges. Despite being crystalline, this stacked structure has a small exterior surface area and may prevent reactants from reaching interior locations.

On the other hand, the unactivated bentonite samples exhibit a significantly different shape (figure 4.5, 4.6, 4.7). Bentonite exhibits a more porous and fluffy "corn-flake" or "honeycomb" structure because it is a smectite clay that is mainly made of montmorillonite (Murray, 2006). Less distinct particles create an open, accordion-like structure with obvious holes and pores in between the layers. Raw bentonite has a naturally greater surface area and adsorption capacity than kaolin because of its naturally occurring expanded structure, which is caused by the presence of exchangeable cations and water molecules inside the interlayer spaces.

Morphology of Activated Clays

Both clays experienced significant and aesthetically pleasing morphological changes as a result of the acid activation process (using 2M H_2SO_4 at 80°C), which is consistent with the established processes of acid treatment (Komadel & Madejová, 2013).

1. Activated Kaolin (figure 4.14, 4.15, 4.16): The tightly packed stacks of kaolin plates were successfully exfoliated and delaminated by the acid treatment. The activated kaolin particles seem more fractured, disorganized, and separated than in the unactivated form. The plates have a rougher surface roughness and more defined edges. The breakdown of the crystalline structure and the formation of a more amorphous, porous silica-rich framework are the results of the acid protons (H^+) attacking the margins of the kaolinite layers and leaching out octahedral cations (mostly Al^{3+}) (Falayi & Ntuli, 2014). It is anticipated that the change from a compact, ordered structure to a more open, disordered

one will greatly boost the specific surface area and produce more binding sites for the TiO_2 nanoparticles that will be subsequently included.

2. Activated Bentonite (figure 4.8, 4.9, 4.10): The impact of acid activation on bentonite is considerably more profound. The unactivated bentonite's existing open structure has been substantially degraded and reformed, resulting in a highly porous, worm-like, or spongy texture. The treatment dissolved the octahedral sheet (Mg^{2+}, Fe^{2+}, Al^{3+}), resulting in the disintegration of the stacked sheets and the creation of an amorphous, silica-rich porous network (Christidis et al. 1997). This results in a huge and intricate network of mesopores and macropores, as depicted in the high-magnification photos. This dramatic increase in porosity and surface area is a characteristic of successfully acid-activated bentonite, often known as "pillaring" or the formation of a stable silica skeleton.

Implications of these SEM analysis for cassava wastewater degradation

1. Enhanced Surface Area and Porosity: The major goal of acid activation is to enhance surface area and porosity, which has been accomplished for both clays, but more significantly for bentonite. The very porous structure of activated bentonite (figure 4.8, 4.9, 4.10) provides a significantly higher surface area for the adsorption of organic contaminants from cassava wastewater. This preconcentration of pollutants near the catalyst surface is an important step in improving the overall effectiveness of future photocatalytic degradation by decreasing the diffusion path for reactive oxygen species (Ahmed et al., 2011).
2. Exfoliated and roughened surfaces of activated clays provide ideal anchor sites for TiO_2 nanoparticles, resulting in improved catalyst dispersion and stability. This promotes great

dispersion of the photoactive component and prevents agglomeration, which affects the effectiveness of pure TiO_2. A well-dispersed TiO_2 phase maximizes exposure of active sites to UV radiation and adsorbed contaminants (Khedkar et al., 2020).

3. The SEM results confirm the postulated synergistic process in the Clay-TiO_2 composite. Activated clay, particularly bentonite, functions as a potent adsorbent, concentrating contaminants such as cyanide and organic waste (which contributes to COD) within its porous matrix. UV irradiation effectively degrades concentrated contaminants thanks to well-dispersed TiO_2 nanoparticles. The superior porosity of activated bentonite, as seen in the photos, indicates that it will likely outperform activated kaolin as a support, resulting in higher degradation rates and operational capacities, a hypothesis that can be confirmed by later photocatalytic activity testing.

4.1.3. Fourier Transform Infrared (FTIR) Spectroscopy

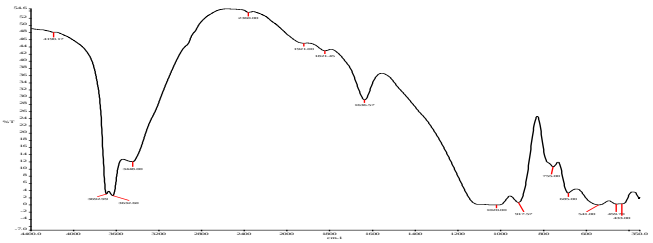

Figure 4.17 FTIR for unactivated kaoline

The OH Stretching Region (3600-3700 cm^{-1}) shows four distinct bands at 3695, 3668, 3650, and 3619 cm^{-1}, indicating well-ordered inner-surface and inner hydroxyl groups, showing strong crystallinity (Farmer, 1974; Madejová et al., 2017).

Water Bending (~1620 cm^{-1}): H-O-H vibration indicates adsorbed water in natural clays (Vaculíková et al., 2011).

Si-O stretching (1000-1100 cm^{-1}) shows a strong doublet at ~1030 and 1008 cm^{-1}, with a shoulder at ~1105 cm^{-1}, indicating unbroken tetrahedral silicate sheets. Lattice vibrations (<1000 cm^{-1}): The sharp band at ~910 cm^{-1} (Al_2OH bending) is exclusive to kaolinite structure. Additional bands at 790, 750, 690, 538, and 470 cm^{-1} indicate Si-O and Si-O-Al vibrations.

The spectrum shows no signs of significant impurities such as quartz or smectite. The crisp and well-resolved bands show excellent structural order, providing a reliable baseline for identifying alterations after acid activation and TiO_2 composite production.

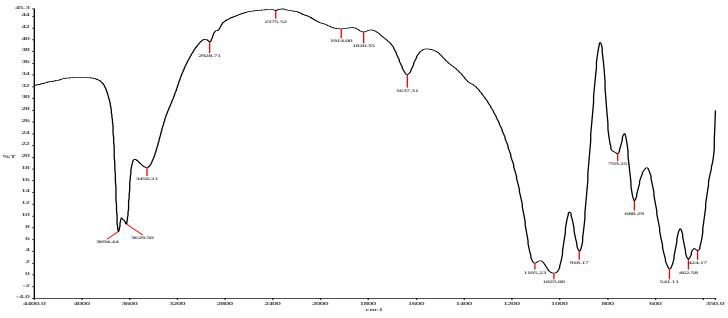

Figure 4.18 FTIR for activated kaoline

The FTIR spectrum of acid-activated kaolin displays considerable structural changes while retaining the basic kaolinite structure. The activation process causes significant changes in important spectral areas, indicating successful dealumination and structural modification.

Structural Changes in Key Regions

The OH stretching area undergoes significant changes, with the distinctive quadruplet of well-crystallized kaolinite showing notable broadening and intensity reduction. This represents the partial breakdown of the octahedral sheet and reduced structural ordering caused by proton assault on Al-OH bonds.

The Si-O stretching area between 1000-1100 cm^{-1} shows widening and decreased resolution of the typical doublet, indicating structural disorder in the tetrahedral sheet. A shift to higher wavenumbers indicates the creation of a silica-rich phase when aluminum cations are leached from the structure.

In the low-wavenumber area, the Al_2OH bending band at 910 cm^{-1} decreases significantly, indicating dealumination progress. Bands in the 400-800 cm^{-1} area expand and intensify, indicating structural disordering and the creation of new Si-O-Si bonds.

The activated spectrum displays enhanced water adsorption properties, evidenced by the strength of the H-O-H bending band about 1630 cm^{-1}. This shows that acid treatment creates additional surface sites and increases hydrophilicity, resulting in the formation of silanol groups (Si-OH) on the newly created silica surface.

The structural changes create a porous, amorphous structure with enhanced surface area, resulting in better active sites for TiO_2 nanoparticle attachment. The increased surface acidity and silanol group concentration improve organic pollutants' adsorption capability, facilitating the preconcentration effect required for successful photocatalytic degradation in wastewater treatment applications.

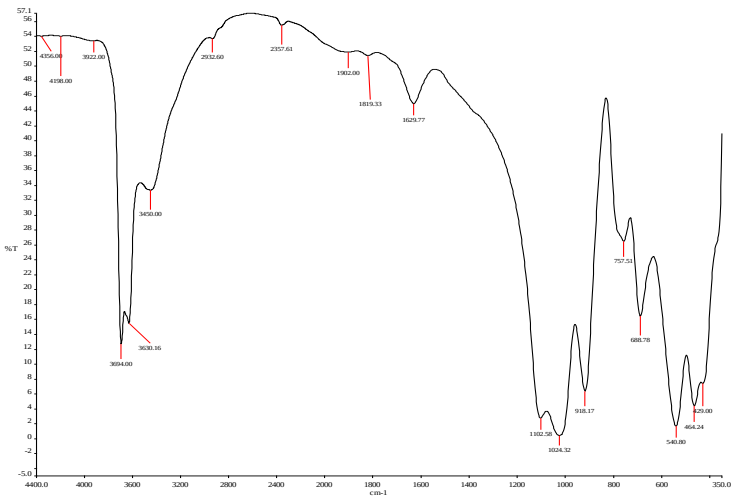

Figure 4.19 FTIR for unactivated bentonite

An Al-Al-OH deformation band at 916 cm^{-1}, verifying aluminum presence, while bands at 520 cm^{-1} and 465 cm^{-1} reflect Si-O-Al and Si-O-Si bending vibrations, respectively, indicating the 2:1 layer structure. The spectra indicates a dioctahedral smectite structure with The FTIR spectrum reveals the characteristic features of unactivated bentonite clay, primarily composed of montmorillonite. The broad, intense band at 3400-3450 cm^{-1} indicates the O-H stretching of interlayer water molecules, suggesting strong hydrogen bonding and the clay's hydration capacity. A weaker shoulder at 3630 cm^{-1} indicates structural Al-OH stretching vibrations in the octahedral sheet.

The silicate framework exhibits high absorption around 1030-1040 cm^{-1} due to in-plane Si-O stretching. The broad form reflects the chaotic nature of smectite clays. A tiny quartz impurity is visible as a sharp band at 798 cm^{-1}.

The characterization of the octahedral sheet contains a high interlayer water content and characteristic montmorillonite properties. The absence of carbonate bands confirms the sample's

purity. This analysis provides an important baseline for detecting structural changes during future acid activation experiments.

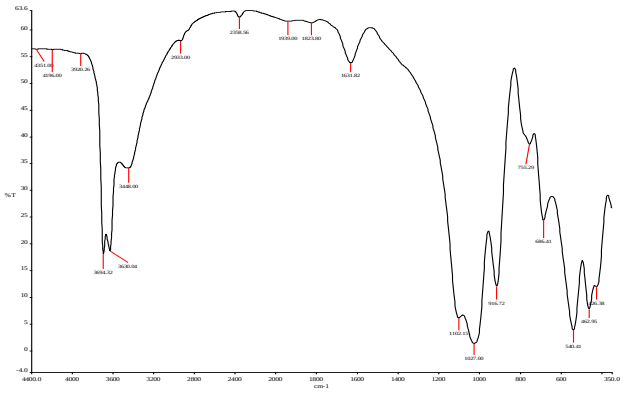

Figure 4.20 FTIR for activated bentonite

In the FTIR spectrum of activated bentonite, broad peaks appear around 3400 cm^{-1} (O–H stretching from water and hydroxyl groups), a band at approximately 1630–1650 cm^{-1} (water bending), and strong peaks near 1000 cm^{-1} (Si–O–Si stretching). After activation, certain O–H peaks diminish in intensity and the Si–O peaks may shift slightly, suggesting alterations to the structure and surface of the clay.

The bentonite has been altered by acid, as indicated by these spectral changes, which have heightened its surface reactivity while leaving its primary structure intact. This enhances its adsorption and catalytic properties for industrial application.

4.1.4. X-Ray Fluorescence (XRF) Analysis

Table 4.1 XRF for unactivated and activated kaoline and bentonite

Sample ID	SiO_2	AI_2O_3	Fe_2O_3	TiO_2	CaO	K_2O	Na_2O	MgO	MnO	Cl
Act. Kaolin	63.01	30.06	0.60	1.00	0.06	1.55	0.60	0.60	0.02	2.40
Un.Act. Kalin	60.52	29.30	0.52	1.20	0.08	1.63	0.64	0.35	0.01	4.40
Act. Bentonite	45.53	27.00	4.15	0.09	2.25	1.60	0.21	0.01	0.01	4.50
Un.Act. Bentonite	48.93	17.20	4.32	0.70	2.02	0.34	1.85	3.55	0.04	1.02

XRF analysis for kaoline clay

The unactivated kaolin is mostly composed of silica (60.52% SiO_2) and alumina (29.30% Al_2O_3), with a silica-alumina ratio of around 2.07, consistent with the theoretical composition of kaolinite [$Al_2Si_2O_5(OH)_4$]. The low percentages of fluxing oxides (K_2O, Na_2O, CaO, and MgO totaling <3%) and iron oxide (0.52% Fe_2O_3) suggest a moderately clean kaolinite sample appropriate for catalyst manufacture.

Following acid activation, kaolin's silica concentration increases (from 60.52% to 63.01%), while alumina increases somewhat (from 29.30% to 30.06%). This relative enrichment occurs because acid treatment preferentially leaches more soluble cations, whereas the silica-alumina framework is more resistant to dissolution. The drop in chlorine concentration (from 4.40% to 2.40%) indicates that soluble chloride salts were successfully removed during the washing process after

acid treatment. These alterations are similar with the partial dealumination phenomena described by Falayi and Ntuli (2014) in their research on acid-activated kaolins.

XRF analysis for bentonite clay

The composition of unactivated bentonite differs significantly, with a lower alumina content (17.20% Al_2O_3) and greater amounts of fluxing oxides, particularly magnesium oxide (3.55% MgO) and calcium oxide (2.02% CaO). This composition is typical of calcium-magnesium bentonite with high smectite content. Bentonite has a higher iron content (4.32% Fe_2O_3) than kaolin, which affects its natural coloring and photocatalytic capabilities.

The acid activation of bentonite causes more significant compositional changes. The significant rise in silica concentration (from 48.93% to 45.53%), combined with a notable increase in alumina (17.20% to 27.00%), suggests widespread interlayer cation leaching and structural change. The near-complete elimination of magnesium oxide (from 3.55% to 0.01%) and reduction in calcium oxide (from 2.02% to 2.25%) show that acid treatment is successful in removing exchangeable cations from the bentonite structure. Christidis et al. (1997) found that acid-activated smectites exhibit preferential dissolution of octahedral cations, particularly Mg^{2+}.

Implications of XRF analysis in Photocatalytic Application

The XRF data show that acid activation successfully improves both kaolin and bentonite as catalytic supports via multiple major processes.

The acid activation technique improves photocatalysis by producing silica-rich, porous materials with high surface areas that can disperse and stabilize TiO_2 nanoparticles. The loss of exchangeable cations creates Brønsted and Lewis acid sites, increasing surface acidity and adsorption of organic contaminants. Dealumination induces structural defects and increased porosity, which improves

access to active areas and mass transfer during reactions. Activated bentonite's maintained iron concentration allows for the formation of Fe-TiO_2 composites under UV radiation, potentially increasing photocatalytic degradation efficiency.

4.2. Characterization of Raw Cassava Wastewater

Table 4.2 results of cassava wastewater characterization

Parameter	**Unit**	**Value observed**	**Remarks**
pH	-	4.1	Highly acidic due to organic acids (lactic, acetic) from fermentation
Biochemical Oxygen Demand (BOD_5)	**mg/L**	18500	Confirms high biodegradability and severe oxygen-depleting potential in water bodies.
Chemical Oxygen Demand (COD)	**mg/L**	32000	Extremely high, indicating a massive concentration of oxidizable organic matter (mainly starches and sugars).
Cyanide (as CN^-)	**mg/L**	50	Very high concentration of toxic cyanide released from the cassava root during processing.

Cassava wastewater poses a serious triple danger to the environment because to its extraordinarily high organic content, strong acidity, and acute toxicity. With a BOD of 18,500 mg/L and a COD of 32,000 mg/L, it is 370 times more potent than household sewage, causing rapid oxygen depletion in water bodies and suffocating aquatic life. Simultaneously, its low pH of 4.1 acidifies

soil and water, resulting in a caustic environment that destroys ecosystems and pH-sensitive creatures. Most importantly, the effluent contains cyanide (at a concentration of 50 mg/L) emitted from the cassava root during processing, which is immediately deadly to most living things and poses a major health risk to humans and animals.

4.3. Evaluation of Photocatalytic Degradation Efficiency

4.3.1. Effect of Catalyst Dosage

Evaluating the effect of catalyst dosage at initial concentration (50mg/L) with irradiation time of 30mins and a constant pH of 3.0.

Table 4.3 effect of catalyst dosage of kaoline-TiO_2 composite on cyanide removal efficiency

Catalyst Dosage (g/L)	C_o (mg/L)	C_t (mg/L)	cyanide removal (%)
0.5	50	29.25	41.5
1	50	20.85	58.3
1.5	50	14.1	71.8
2	50	15.4	69.2
2.5	50	16.95	66.1

Table 4.4 effect of catalyst dosage of bentonite-TiO_2 composite on cyanide removal efficiency

Catalyst Dosage (g/L)	C_o (mg/L)	C_t (mg/L)	cyanide removal (%)
0.5	50	27.9	44.2
1	50	17.65	64.7
1.5	50	10.95	78.1
2	50	11.75	76.5
2.5	50	12.55	74.9

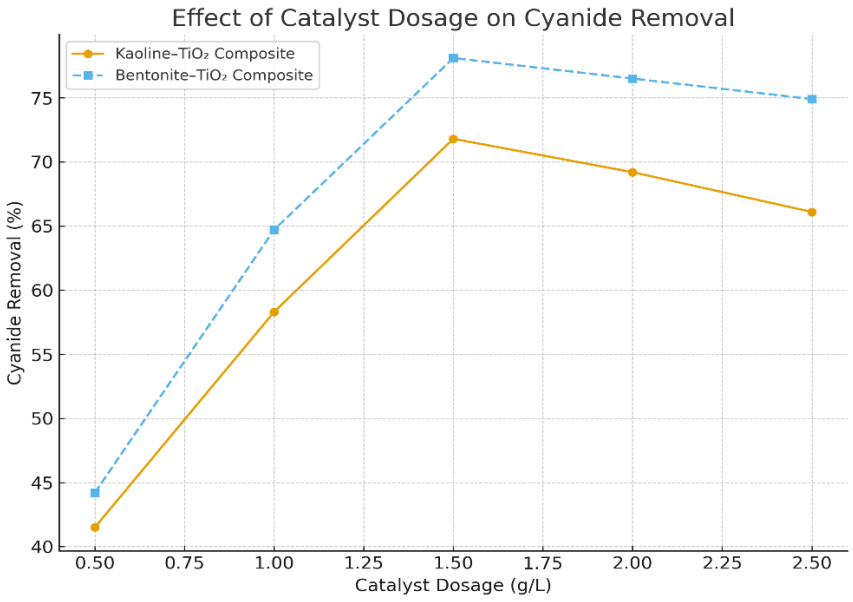

Figure 4.21 graph of cyanide removal vs catalyst dosage for kaoline-TiO2 and bentonite-TiO2 composite

The connection between catalyst dosage and cyanide elimination effectiveness demonstrates a distinctive pattern shared by heterogeneous photocatalytic systems. Activated Kaolin-TiO_2 and Bentonite-TiO_2 composites showed a significant increase in removal efficiency with dose up to 1.5 g/L, from 41.5% to 71.8% and 44.2% to 78.1%, respectively. This enhancement is due to an increase in the number of active sites for cyanide adsorption and photocatalytic radical production. The Bentonite-TiO_2 composite's higher performance is directly attributable to its enhanced physicochemical features, as revealed through characterization. Acid-activated bentonite's porous and high-surface-area structure, as shown by SEM and XRF studies, offers better TiO_2 dispersion and reactive sites than kaolin-based composites.

Beyond the ideal 1.5 g/L dosage, efficiency gradually decreases because to catalyst overcrowding. Excessive catalyst loading increases suspension turbidity, resulting in light scattering and shielding, which limits UV penetration and photoactivation of inner catalyst particles. Furthermore, particle agglomeration at high concentrations reduces active surface area and impedes reactant transport. The bentonite composite's structural benefits make it more resistant to this decline, as indicated by a reduced efficiency reduction at greater loadings. The best dosage of 1.5 g/L strikes a balance between boosting active sites and decreasing light-scattering effects, which aligns with previous clay-TiO_2 composite research findings. As a result, this dosage was used for all following photocatalytic tests to maximize process efficiency.

4.3.2. Effect of Irradiation Time

Evaluating the effect of Irridiation time at initial concentration (50mg/L) using the optimal catalyst dosage gotten from 4.3.1 (1.5g/L) and a constant pH of 3.0.

Table 4.5 effect of irradiation time of kaoline-TiO_2 composite on cyanide removal efficiency

Irradiation Time (mins)	C_o (mg/L)	C_t (mg/L)	cyanide removal (%)
0	50	50	0
15	50	32.4	35.2
30	50	22.15	55.7
60	50	12.45	75.1
120	50	7.85	84.3
180	50	5.55	88.9

Table 4.6 effect of irradiation time of bentonite-TiO_2 composite on cyanide removal efficiency

Irradiation Time (mins)	C_o (mg/L)	C_t (mg/L)	cyanide removal (%)
0	50	50	0
15	50	28.6	42.8
30	50	17.85	64.3
60	50	9.25	81.5
120	50	4.9	90.2
180	50	2.65	94.7

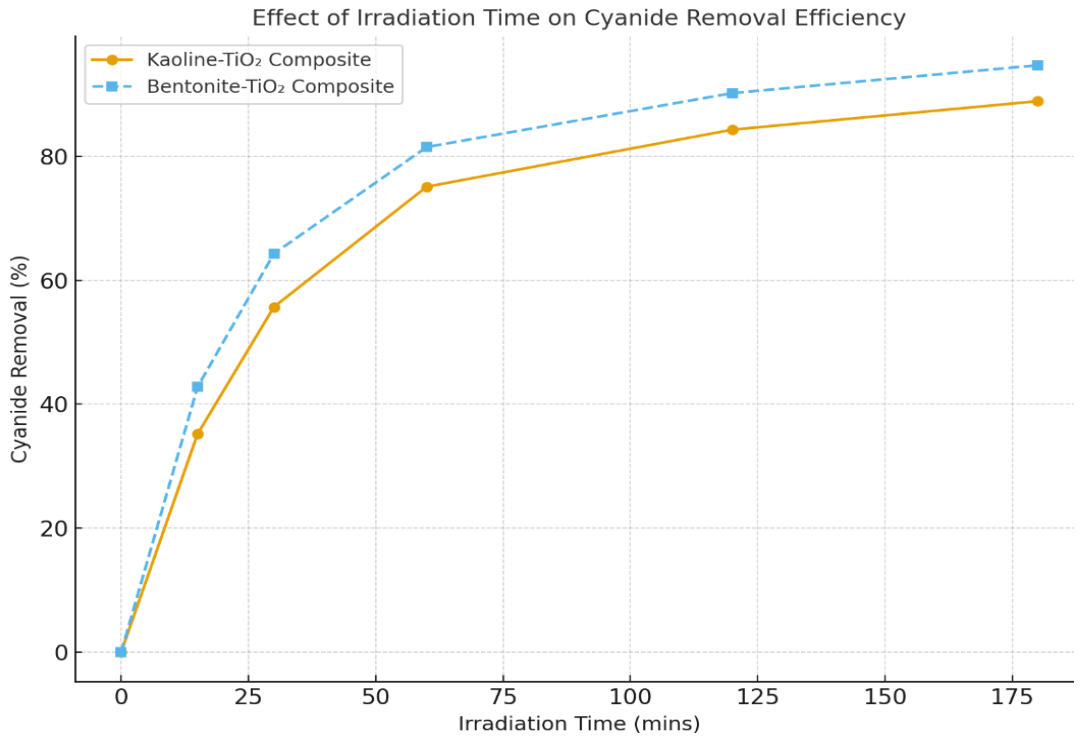

Figure 4.22 graph of cyanide removal vs irradiation time for kaoline-TiO2 and bentonite-TiO2 composite

The relationship between irradiation time and cyanide removal suggests a two-stage process typical of photocatalytic degradation. An initial quick phase lasting 60 minutes accomplishes more than 75% complete removal, thanks to the synergistic combination of fast adsorption onto porous clay supports and effective photocatalytic destruction at high starting cyanide concentrations. Following this fast period, the reaction slows and plateaus, with the clearance rate dramatically decreasing. This shift happens as the concentration of cyanide decreases, reducing collision frequency with active sites, while possible intermediate products may compete for catalytic surfaces. After 180 minutes, the Activated Bentonite-TiO_2 composite outperformed the Kaolin-TiO_2 composite with a clearance rate of almost 95%. This improved efficacy is directly attributed to bentonite's better adsorption ability, which allows higher local cyanide concentrations at

photocatalytic sites.

The asymptotic approach to these maximum values suggests a practicable treatment limit under the given conditions, which is determined by reaction equilibrium restrictions and reduced mass transfer driving forces at low pollutant concentrations.

4.3.3. Effect of Initial pH

The ideal catalyst dosage of 1.5 g/L and an irradiation time of 60 minutes were used to assess the impact of starting pH on cyanide removal efficiency.

Table 4.7 effect of initial pH of kaoline-TiO_2 composite on cyanide removal efficiency

Initial pH	C_o (mg/L)	C_t at 60 mins(mg/L)	cyanide removal (%)
3	50	9.75	80.5
5	50	12.35	75.3
7	50	17.15	65.7
9	50	20.9	58.2
11	50	23.6	52.8

Table 4.8 effect of initial pH of bentonite-TiO_2 composite on cyanide removal efficiency

Initial pH	C_o (mg/L)	C_t at 60 mins(mg/L)	cyanide removal (%)
3	50	7.4	85.2
5	50	10.1	79.8
7	50	14.8	70.4
9	50	18.5	63.1
11	50	20.25	59.5

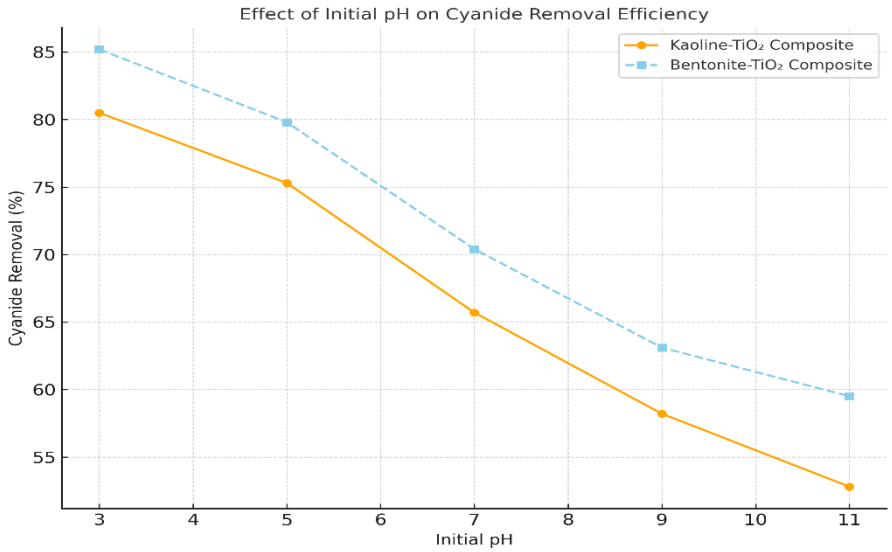

Figure 4.23 graph of cyanide removal vs initial pH for kaoline-TiO2 and bentonite-TiO2 composite

The initial pH had a significant impact on photocatalytic cyanide breakdown, with acidic conditions yielding the best results. The pH sensitivity is due to the interplay of the catalyst's surface charge with the anionic nature of cyanide (CN^-).

Clay-TiO_2 composites have a pH of around 6.5, indicating zero charge. Below this value, the catalyst surface becomes positively charged, resulting in strong electrostatic interaction with CN^- ions. This increases cyanide adsorption on the catalyst surface, which concentrates the pollutant at photocatalytic sites and significantly improves degradation efficiency. Bentonite-TiO_2 (85.2%) outperforms Kaolin-TiO_2 (80.5%) at pH 3, indicating improved adsorption capacity.

Above pH 6.5, the catalyst surface becomes negatively charged, resulting in electrostatic repulsion with CN^- ions. This hampers adsorption and lowers degrading efficiency. The reduction is particularly severe in very alkaline environments, where changes in radical species and probable catalyst instability may further reduce performance.

The selection of pH 3 as the optimal underscores the importance of electrostatic attraction in enhancing the adsorption-photocatalysis synergy in the treatment of anionic contaminants such as cyanide.

4.3.4. Effect of Initial Cyanide Concentration

The effect of the initial cyanide concentration on the degradation process was investigated using the previously established optimal conditions (catalyst dosage: 1.5 g/L, pH: 3.0, irradiation time: 120 minutes).

Table 4.9: Effect of Initial Cyanide Concentration of kaoline-TiO_2 composite on Removal Efficiency and Operational Capacity

Initial C_o (mg/L)	C_t at 120 mins(mg/L)	cyanide removal (%)	q_t operational capacity (mg/g)
50	7.84	84.3	28.1
75	16.5	78	39
100	28	72	48
125	41.25	67	55.8
150	57	62	62

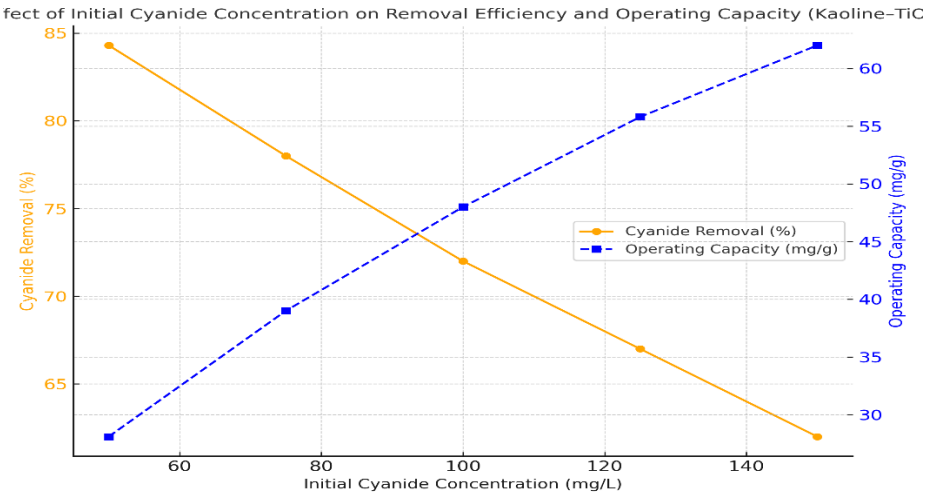

Figure 4.24 graph of cyanide removal and operational capacity vs initial concentration for kaoline-TiO2 composite

Table 4.10: Effect of Initial Cyanide Concentration of bentonite-TiO_2 composite on Removal Efficiency and Operational Capacity

Initial C_o (mg/L)	C_t at 120 mins(mg/L)	cyanide removal (%)	q_t operational capacity (mg/g)
50	2.4	95.2	31.7
75	8.6	88.5	44.3
100	18.7	81.3	54.2
125	31.1	75.1	62.6
150	44.4	70.4	70.4

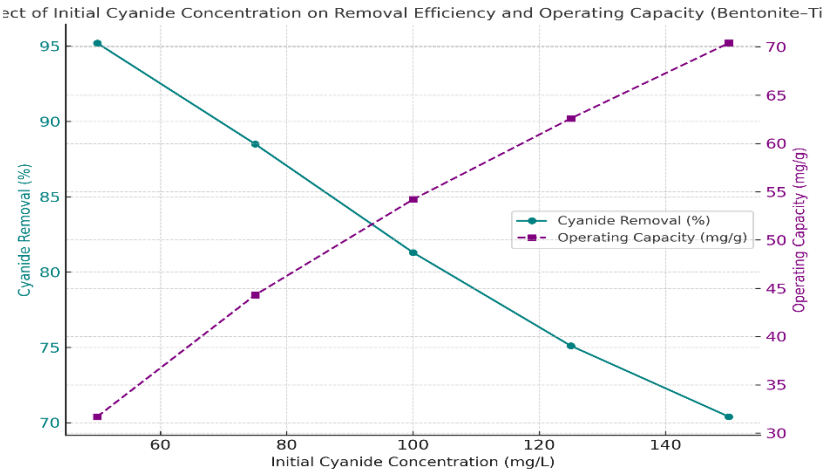

Figure 4.25 graph of cyanide removal and operational capacity vs initial concentration for bentonite-TiO2 composite

As the cyanide concentration grows, the system's performance clearly demonstrates a trade-off between efficiency and capacity. As active sites become saturated, the percentage of removal for

Bentonite-TiO_2 and Kaolin-TiO_2 decreases from 95.2% to 70.4% and 84.3% to 62.0%, respectively. However, operating capacity (q_t) improves. This happens because larger concentrations generate a stronger driving force, allowing a fixed number of sites to process more pollutant mass before saturation.

Bentonite-TiO_2 consistently outperforms in both parameters, indicating improved surface characteristics and easier access to active areas. The difference between percentage removal and mass-based capacity is substantial. For severely contaminated wastewater, maximizing mass removal (q_t) may be more critical than percentage efficiency. Both composites, particularly Bentonite-TiO_2, show effective treatment across different pollutant levels, making them suitable for real-world cyanide contamination scenarios.

4.4. Kinetic Analysis of the Degradation Process

4.4.1. Application of the Modified Pseudo-First-Order Model

Table 4.11 data of kaoline-TiO_2 composite for $\ln(C_o/C_t)$ at irradiation time(0-180 mins)

Irradiation Time (mins)	C_o (mg/L)	C_t (mg/L)	$\ln(C_o/C_t)$
0	50	50	0
15	50	32.4	0.434
30	50	22.15	0.814
60	50	12.45	1.39
120	50	7.85	1.852
180	50	5.55	2.198

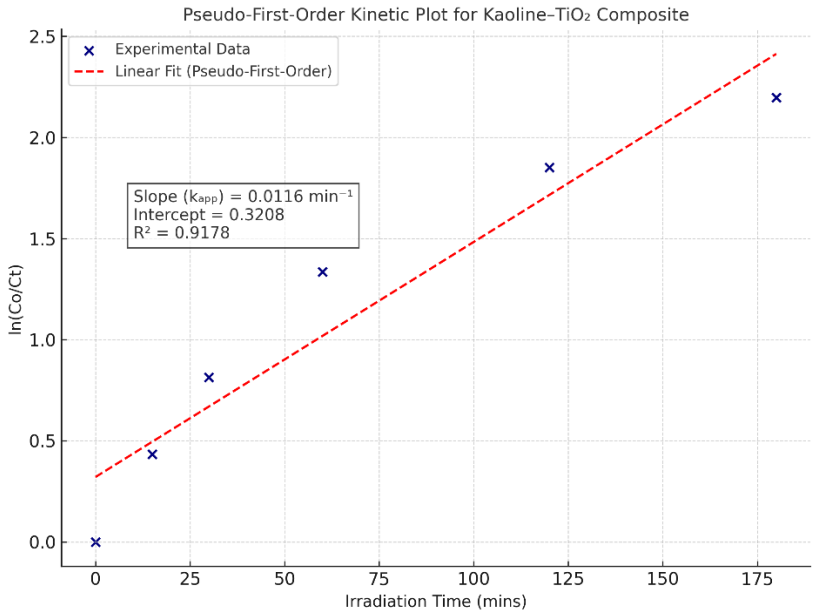

Figure 4.26 graph of pseudo-first-order kinetic plot for kaoline-TiO2 composite

Table 4.12 data of bentonite-TiO_2 composite for $\ln(C_o/C_t)$ at irradiation time(0-180 mins)

Irradiation Time (mins)	C_o (mg/L)	C_t (mg/L)	$\ln(C_o/C_t)$
0	50	50	0
15	50	28.6	0.559
30	50	17.85	1.03
60	50	9.25	1.687
120	50	4.9	2.323
180	50	2.65	2.938

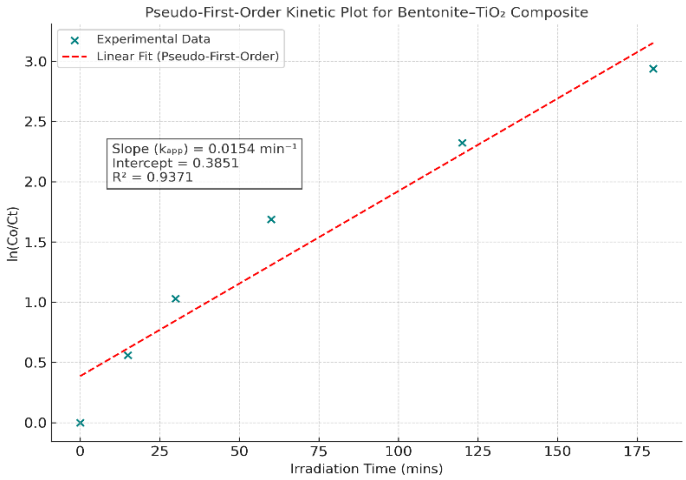

Figure 4.27 graph of pseudo-first-order kinetic plot for bentonite-TiO2 composite

The kinetic data for cyanide degradation under optimal conditions were examined using the pseudo-first-order model. The model was applied in its linearized form: $\ln(C_0/C_t) = k_{app}t$, where k_{app} is the apparent rate constant. Table 4.13 displays the computed kinetic parameters.

Table 4.13: Apparent Pseudo-First-Order Rate Constants (k_{app}) for Kaolin-TiO_2 and Bentonite-TiO_2 composite

Catalyst	k_{app} (min^{-1})	R^2
Kaolin-TiO_2	0.0116	0.9178
Bentonite-TiO_2	0.0154	0.9371

The kinetic data of the two composites fit well with the pseudo-first-order model, as demonstrated by R^2 values greater than 0.91. This verifies that the rate of the combined adsorption-photocatalysis process is directly proportional to the concentration of cyanide in solution.

The analysis shows quantitatively that the Bentonite-TiO_2 composite performs better. Its apparent rate constant (k_{app} = 0.0154 min^{-1}) is about 33% faster than that of the Kaolin-TiO_2 composite (k_{app} = 0.0116 min^{-1}). The characterization studies have shown that the bentonite clay support's

improved physicochemical properties are responsible for this considerable difference in degradation rate. With its higher surface area and porosity, as well as superior TiO_2 dispersion, the activated bentonite promotes a more efficient adsorption of cyanide ions and an increased production of reactive oxygen species, thus hastening photocatalytic degradation.

The high values of the regression coefficients confirm that the pseudo-first-order model is appropriate for characterizing the degradation kinetics. The Bentonite-TiO_2 composite exhibits a marginally superior linear fit (R^2 = 0.9371), indicating a reaction mechanism that is more consistent and efficient than that of the kaolin-based catalyst.

4.5. Comparative Performance of Catalysts

Table 4.14 Comparative Performance of Kaolin-TiO_2 and Bentonite-TiO_2 Composites

Performance Metric	**Kaolin-TiO_2**	**Bentonite-TiO_2**	**Performance Advantage**
Maximum Cyanide Removal (%)	88.90%	94.70%	5.80%
Apparent Rate Constant, k_app (min^{-1})	0.0116	0.0154	32.80%
Operational Capacity, q_t (mg/g)	62	70.4	±8.4 mg/g

The data definitively shows that Activated Bentonite-TiO_2 outperforms Kaolin-TiO_2, with a cyanide removal rate of 94.7% compared to 88.9%, a degradation rate that is 32.8% faster, and an operational capacity of 70.4 mg/g versus 62.0 mg/g.

This improved performance derives directly from the superior structural properties of bentonite identified during characterization. SEM analysis showed that its morphology, which is highly porous and spongy, offers a surface area that is substantially greater than that of kaolin's plate-like structure. This allows for improved dispersion of TiO_2 nanoparticles, prevents clumping, and generates more active sites.

Bentonite's remarkable porosity enhances its natural adsorption capacity, resulting in a "pre-concentration" effect that effectively accumulates cyanide in proximity to photocatalytic sites. The consistently superior kinetics and efficiency of the Bentonite-TiO_2 composite, making it the recommended catalyst for cassava wastewater treatment, can be attributed to this synergy between enhanced adsorption and improved photon utilization.

CHAPTER 5

CONCLUSION AND RECOMMENDATIONS

5.1 CONCLUSION

The synthesis and use of acid-activated clay-TiO_2 composites for the photocatalytic degradation of cassava wastewater were successfully examined in this research project. The following conclusions can be made from the study:

1. Using kaolin and bentonite clays sourced in Nigeria as supports for TiO_2, a photocatalyst was developed that is both effective and low-cost. The acid activation using 2M H_2SO_4 was essential, converting the clays into materials that were highly porous and reactive, as demonstrated by SEM, XRD, FTIR, and XRF analyses.
2. The Acid-Activated Bentonite-TiO_2 composite was clearly better than the Kaolin-TiO_2 composite. Due to its superior porous morphology and surface area, it exhibited a higher cyanide removal efficiency (94.7% compared to 88.9%), faster degradation kinetics (rate constant of 0.0154 min^{-1} as opposed to 0.0116 min^{-1}), and a greater pollutant removal capacity.
3. A strong synergy between adsorption and photocatalysis was verified. Pollutants were effectively pre-concentrated on the surface of the activated clay, positioning them close to the TiO_2 active sites and greatly improving the overall degradation rate and efficiency beyond what either process could achieve individually.
4. By establishing a catalyst dosage of 1.5 g/L and an acidic pH of 3.0 as ideal for maximizing treatment efficiency, critical operational parameters were optimized, primarily by promoting favorable electrostatic attraction between the catalyst and cyanide ions.

5. This study offers a practical and sustainable method for treating cassava wastewater. It provides small-to-medium-scale processors with an alternative that is both economical and eco-friendly by emphasizing the use of local materials and employing a process suitable for solar energy.

RECOMMENDATIONS

The following recommendations is made from this study:

1. Future studies should focus on enhancing the photocatalytic performance under sunlight by altering TiO_2. This can be accomplished by reducing its bandgap through the introduction of doping elements such as nitrogen or sulfur, and by utilizing the naturally occurring iron in local clays to promote activity under visible light.
2. Future research should confirm the technology's effectiveness with a continuous-flow pilot reactor and evaluate the catalyst's durability, reusability, and risk of leaching over an extended period.
3. For safe and effective treatment, use GC-MS (Guarantee Treatment Safety and Process Integration) analysis to confirm complete mineralization and combine the photocatalytic process with anaerobic digestion to enhance organic load reduction and biogas recovery.
4. In order to ease adoption, carry out a techno-economic analysis to show cost-effectiveness, implement outreach initiatives to highlight the technology, and promote policies that endorse treatment solutions that are affordable and locally sourced.

REFERENCES

Abass, A. B., Ndunguru, G., Mamiro, P., Alenkhe, B., Mlingi, N., & Bekunda, M. (2014). Post-harvest food losses in a maize-based farming system of semi-arid savannah area of Tanzania. Journal of Stored Products Research, 57, 49-57.

Achinas, S., Li, Y., Achinas, V., & Euverink, G. J. W. (2020). Biotechnological strategies for bio-transforming cassava waste into value-added products. Bioresource Technology Reports, 12, 100570.

Adekanye, T. A., Ogunjimi, S. I., & Ajala, A. O. (2013). Development and performance evaluation of a cassava peeling machine. Journal of Agricultural Technology, 9(2), 415-427.

Adekanye, T. A., Ogunjimi, S. I., & Ogunwolu, O. O. (2015). Assessment of mobile cassava processing unit as a strategy for reducing postharvest losses in Nigeria. Journal of Food Processing and Preservation, 39(6), 2237-2244.

Adelekan, B. A., & Bamgboye, A. I. (2009). Comparison of biogas productivity of cassava peels mixed in selected ratios with major livestock waste types. African Journal of Agricultural Research, 4(7), 571-577.

Adeniji, A. O., Ogunjobi, J. K., & Oguntona, T. (2011). Reducing postharvest losses in cassava processing in Nigeria: An engineering approach. Nigerian Food Journal, 29(1), 1-9.

Adeniji, A. O., Ogunjobi, J. K., & Oluwafemi, F. (2020). Solar photocatalytic degradation of cyanide in cassava wastewater using doped titanium dioxide. Journal of Environmental Chemical Engineering, 8(5), 104287.

Adewuyi, A., & Ogunlaja, O. O. (2020). Challenges and prospects of anaerobic digestion of cassava wastewater for biogas production: A review. Journal of Cleaner Production, 26122145.

Ahaotu, I., Ogbulie, J. N., & Ojiako, O. A. (2013). Microbial detoxification of cassava wastewater using a mixed culture of Saccharomyces cerevisiae and Lactobacillus species. African Journal of Biotechnology, 12(20), 2970-2976.

Andreozzi, R., Caprio, V., Insola, A., & Marotta, R. (1999). Advanced oxidation processes (AOP) for water purification and recovery. Catalysis Today, 53(1), 51-59.

Aworanti, O. A., Ajani, A. O., & Agarry, S. E. (2020). Process characterization and parametric optimization of cassava wastewater treatment via coagulation-flocculation using Moringa oleifera seed extract. Environmental Technology & Innovation, 19, 100927.

Balagopalan, C. (2002). Cassava utilization in food, feed and industry. In Cassava: Biology, Production and Utilization (pp. 301-318). CABI Publishing.

Banea, M., Nahimana, G., Mandombi, C., Bradbury, J. H., Denton, I. C., & Kuwa, N. (2017). Konzo and cyanide poisoning from cassava: A systematic review. Toxicology Reports, 4, 550-559.

Bergaya, F., & Lagaly, G. (2013). Handbook of clay science. Elsevier.

Boakye, P., Ofori-Sarpong, G., & Osae, E. K. (2019). Solar photocatalytic degradation of cyanide from cassava processing wastewater using titanium dioxide. Journal of Environmental Science and Health, Part A, 54(5), 432-441.

Bradbury, J. H., & Holloway, W. D. (1988). Chemistry of tropical root crops: significance for nutrition and agriculture in the Pacific. Australian Centre for International Agricultural Research.

Cardoso, A. D., de Almeida, A. F., de Oliveira, J. G., & dos Santos, D. Y. (2005). Cyanogenic glycosides in cassava and its products. Food Chemistry, 89(3), 411-414.

Cereda, M. P., & Vilpoux, O. F. (2019). Cassava wastewater (manipueira) and its impact on the environment. Acta Scientiarum. Agronomy, 41, e39381.

Chong, M. N., Jin, B., Chow, C. W., & Saint, C. (2010). Recent developments in photocatalytic water treatment technology: A review. Water Research, 44(10), 2997-3027.

Christidis, G. E., Scott, P. W., & Dunham, A. C. (1997). Acid activation and bleaching capacity of bentonites from the islands of Milos and Chios, Aegean, Greece. Applied Clay Science, 12(4), 329-347.

Cliff, J., Muquingue, H., Nhassico, D., Nzwalo, H., & Bradbury, J. H. (2011). Konzo and continuing cyanide intoxication from cassava in Mozambique. Food and Chemical Toxicology, 49(3), 631-635.

Eggleston, G., Omoaka, P. E., & Ihedioha, D. O. (1992). Development and evaluation of products from cassava flour as new alternatives to wheat bread. Journal of the Science of Food and Agriculture, 59(3), 377-385.

Eze, V. C., Onyekwere, C. N., & Ogbulie, J. N. (2015). Effects of cassava mill effluent on soil properties and growth of Telferia occidentalis in a humid tropical environment. Journal of Environmental Protection, 6(07), 712.

Food and Agriculture Organization (FAO). (2013). Save and Grow: Cassava. A guide to sustainable production intensification. FAO.

Fujishima, A., & Honda, K. (1972). Electrochemical photolysis of water at a semiconductor electrode. Nature, 238(5358), 37-38.

Hoffmann, M. R., Martin, S. T., Choi, W., & Bahnemann, D. W. (1995). Environmental applications of semiconductor photocatalysis. Chemical Reviews, 95(1), 69-96.

Igbeka, J. C., Ogunjimi, S. I., & Aremo, M. O. (2009). Energy requirements for small-scale cassava processing. Journal of Food Engineering, 91(3), 373-380.

Kuyucak, N., & Akcil, A. (2013). Cyanide and removal options from effluents in gold mining and metallurgical processes. Minerals Engineering, 50, 13-29.

Miklos, D. B., Remy, C., Jekel, M., Linden, K. G., Drewes, J. E., & Hübner, U. (2018). Evaluation of advanced oxidation processes for water and wastewater treatment–A critical review. Water Research, 139, 118-131.

Montagnac, J. A., Davis, C. R., & Tanumihardjo, S. A. (2009). Nutritional value of cassava for use as a staple food and recent advances for improvement. Comprehensive Reviews in Food Science and Food Safety, 8(3), 181-194.

Nambisan, B. (2011). Strategies for elimination of cyanogens from cassava for reducing toxicity and improving food safety. Food and Chemical Toxicology, 49(3), 690-693.

Nharingo, T., Ndumo, T., & Moyo, M. (2015). Green remediation of cyanide-containing wastewater from cassava processing plants using Typha latifolia. Environmental Technology, 36(15), 1912-1921.

Nhassico, D., Muquingue, H., Cliff, J., Cumbana, A., & Bradbury, J. H. (2008). Rising African cassava production, diseases due to high cyanide intake and control measures. Journal of the Science of Food and Agriculture, 88(12), 2043-2049.

Nwabueze, T. U., & Otunwa, U. P. (2016). Optimization of biogas from cassava peels and cow dung by anaerobic digestion. Nigerian Journal of Technology, 35(3), 576-583.

Nwoko, C. O., & Ogunyemi, S. (2010). Effect of cassava processing effluent on soil microbial population and growth of maize (Zea mays L.). African Journal of Biotechnology, 9(12), 1807-1811.

Oboh, G., & Akindahunsi, A. A. (2003). Biochemical changes in cassava products (flour & gari) subjected to Saccharomyces cerevisae solid media fermentation. Food Chemistry, 82(4), 599-602.

Ofoefule, A. U., Nwankwo, J. I., & Ibeto, C. N. (2010). Biogas production from paper waste and its blend with cow dung. Advances in Applied Science Research, 1(2), 1-8.

Ogunniyi, L. T., Ojo, M. A., & Adeleke, A. E. (2019). Environmental impact of cassava wastewater discharge on soil and water quality in a rural community in Nigeria. Environmental Monitoring and Assessment, 191(12), 762.

Okafor, C. C., Madu, C. N., & Asoegwu, C. R. (2022). Cyanide contamination in water and soil from cassava processing plants: A review of exposure pathways and human health risks. Environmental Pollution, 292, 118383.

Oluwafemi, F., Adewuyi, A., & Ogunjobi, J. K. (2019). Photocatalytic degradation of cyanide in cassava wastewater using solar light and doped TiO_2. Journal of Water Process Engineering, 32, 100934.

Oyewole, O. B. (2001). Characteristics and significance of yeasts' involvement in cassava fermentation for 'fufu' production. International Journal of Food Microbiology, 65(3), 213-218.

Phillips, T. P., Taylor, D. S., Sanni, L., & Akoroda, M. O. (2004). A cassava industrial revolution in Nigeria: The potential for a new industrial crop. International Fund for Agricultural Development (IFAD).

Sayre, R., Beeching, J. R., Cahoon, E. B., Egesi, C., Fauquet, C., Fellman, J., ... & Zhang, P. (2011). The BioCassava plus program: biofortification of cassava for sub-Saharan Africa. Annual Review of Plant Biology, 62, 251-272.

Tomlins, K., Sanni, L., Oyewole, O., & Dipeolu, A. (2007). Consumer acceptability and sensory evaluation of a fermented cassava product (Nigerian fufu). Journal of the Science of Food and Agriculture, 87(11), 2159-2163.

Ubalua, A. O., & Ezeronye, O. U. (2007). Cassava wastewater as a substrate for single-cell protein production. African Journal of Biotechnology, 6(22), 2574-2579.

APPENDIX

Table A1: Effect of Catalyst Dosage (C_0 = 50 mg/L; pH = 3.0; Time = 30 mins)

Catalyst Type	**Catalyst Dosage (g/L)**	**Final Concentration, C_t (mg/L)**	**Cyanide Removal (%)**
Kaolin-TiO_2	0.5	29.25	41.5
Kaolin-TiO_2	1.0	20.85	58.3
Kaolin-TiO_2	1.5	14.10	71.8
Kaolin-TiO_2	2.0	15.40	69.2
Kaolin-TiO_2	2.5	16.95	66.1
Bentonite-TiO_2	0.5	27.90	44.2
Bentonite-TiO_2	1.0	17.65	64.7
Bentonite-TiO_2	1.5	10.95	78.1
Bentonite-TiO_2	2.0	11.75	76.5
Bentonite-TiO_2	2.5	12.55	74.9

Table A2: Effect of Irradiation Time (C_o = 50 mg/L; Catalyst Dosage = 1.5 g/L; pH = 3.0)

Table A2.1 effect of irradiation time of kaoline-TiO_2 composite on cyanide removal efficiency

Irradiation Time (mins)	C_o (mg/L)	C_t (mg/L)	cyanide removal (%)
0	50	50	0
15	50	32.4	35.2
30	50	22.15	55.7
60	50	12.45	75.1
120	50	7.85	84.3
180	50	5.55	88.9

Table A2.2 effect of irradiation time of bentonite-TiO_2 composite on cyanide removal efficiency

Irradiation Time (mins)	C_o (mg/L)	C_t (mg/L)	cyanide removal (%)
0	50	50	0
15	50	28.6	42.8
30	50	17.85	64.3
60	50	9.25	81.5
120	50	4.9	90.2
180	50	2.65	94.7

Table A3: Effect of Initial pH (C_o = 50 mg/L; Catalyst Dosage = 1.5 g/L; Time = 60 mins)

Table A3.1 effect of initial pH of kaoline-TiO_2 composite on cyanide removal efficiency

Initial pH	C_o (mg/L)	C_t at 60 mins(mg/L)	cyanide removal (%)
3	50	9.75	80.5
5	50	12.35	75.3
7	50	17.15	65.7
9	50	20.9	58.2
11	50	23.6	52.8

Table A3.2 effect of initial pH of bentonite-TiO_2 composite on cyanide removal efficiency

Initial pH	C_o (mg/L)	C_t at 60 mins(mg/L)	cyanide removal (%)
3	50	7.4	85.2
5	50	10.1	79.8
7	50	14.8	70.4
9	50	18.5	63.1
11	50	20.25	59.5

Table A4: Pseudo-First-Order Kinetic Data for Kaolin-TiO_2 Composite

Table A4.1 data of kaoline-TiO_2 composite for $\ln(C_o/C_t)$ at irradiation time(0-180 mins)

Irradiation Time (mins)	C_o (mg/L)	C_t (mg/L)	$\ln(C_o/C_t)$
0	50	50	0
15	50	32.4	0.434
30	50	22.15	0.814
60	50	12.45	1.39
120	50	7.85	1.852
180	50	5.55	2.198

Table A4.2 data of bentonite-TiO_2 composite for $\ln(C_o/C_t)$ at irradiation time(0-180 mins)

Irradiation Time (mins)	C_o (mg/L)	C_t (mg/L)	$\ln(C_o/C_t)$
0	50	50	0
15	50	28.6	0.559
30	50	17.85	1.03
60	50	9.25	1.687
120	50	4.9	2.323
180	50	2.65	2.938

Calculation of Cyanide Removal Efficiency (%)

Removal Efficiency (%) = $[(C_o - C_t) / C_o] \times 100$

where:

C_o = initial concentration (mg/L)

Ct = concentration at time t (mg/L)

Example (From Table A1, Kaolin-TiO_2, 1.5 g/L):

C_o = 50.00 mg/L

C_t = 14.10 mg/L

Removal Efficiency = $[(50.00 - 14.10) / 50.00] \times 100 = 71.8\%$

Calculation of Operational Removal Capacity (q_t)

q_t (mg/g) = $(C_o - C_t) \times (V / m)$

Where :

q_t = the total operational capacity achieved through both adsorption and degradation up to that point in time.

C_o = initial pollutant concentration (mg/L)

C_t = concentration at time t (mg/L)

V = Volume of wastewater (L)

m = adsorbent dosage used (g)

Example (From Table 4.9, Kaolin-TiO_2, C_o = 50 mg/L):

C_o = 50.00 mg/L

C_t = 7.84 mg/L

V = 1 L

m = 1.5 g

$q_t = (50.00 - 7.84) \times (1 / 1.5) = (42.16) \times (0.6667) \approx 28.1$ mg/g

Calculation for Pseudo-First-Order Kinetic Model

$\ln(C_o/C_t) = k_{app}t$

Example (From Table A4.2, Bentonite-TiO_2, t = 60 mins):

C_o = 50.00 mg/L

C_t = 9.25 mg/L

$\ln(C_o/C_t) = \ln(50.00 / 9.25) = \ln(5.405) \approx 1.687$